united nations educational, scientific and cultural organization

international atomic energy agency

the
abdus salam
international centre for theoretical physics

SMR/1328/6

School on the Physics of Equatorial Atmosphere

(24 September - 5 October 2001)

Mean Meridional Circulation and Transport

L. Gray
(Rutherford Appleton Laboratory, UK)

Mean Meridional Circulation and Transport

1. Background

We have seen that the semi annual oscillation (SAO) and the quasi biennial oscillation (QBO) in zonal winds are the result of the interaction of vertically propagating waves with the background flow. There is also a clear SAO / QBO in temperature. The positive correlation between temperature anomalies averaged over the 30-50 hPa layer and the vertical shear in zonal wind over the same layer, taken from Singapore balloon observations (figure 1) shows that the tropical temperature QBO is in thermal wind balance with the vertical shears of the zonal winds:

$$\partial u/\partial z \;\alpha\; -\partial T/\partial y$$

A westerly vertical shear zone is therefore associated with a positive temperature anomaly at the equator and an easterly vertical shear is associated with a negative temperature anomaly. In westerly shear zones the maximum in temperature at the equator is maintained against thermal damping by adiabatic warming due to sinking motion. The opposite holds in easterly shear zones. The pattern of shear zones and meridional circulations is shown schematically in figure 2.

The presence of a warm temperature anomaly at the equator, associated with westerly vertical shear, also gives rise to anomalous radiative cooling, leading to mean sinking (or at least anomalously weak tropical upwelling, since the background flow is strongly upwelling). There may also be a significant radiative feedback of the QBO anomaly in ozone on the induced meridional circulation, since changes in ozone have a direct effect on short-wave heating.

This circulation with rising or sinking at the equator is compensated by an opposing circulation off the equator, which gives rise to (much smaller) anomalies in the subtropics and midlatitudes of opposite sign to that at the equator (see fig. 2).

Figures 3-5 show the latitude time-series at 32 hPa (approx. 24 km) of QBO anomalies in zonal wind, temperature and (residual mean) vertical velocities from meteorological analyses (Randel et al. 1999). The equatorial zonal wind anomalies (figure 3) extend between 20°S – 20°N. The temperature anomalies (figure 4) are in approximate thermal wind balance with the wind anomalies and the timing is determined by the vertical wind shear. There is also evidence of a phase change at around 15° latitude and a weak subtropical anomaly. The north polar signal, which is large (but not so significant statistically due to the large variability in this region) is associated with a QBO modulation of the amplitude and timing of NH stratospheric sudden warmings. The vertical velocities (figure 5) are consistent with the meridional circulation of figure 2, showing a phase change in the subtropics and a smaller return arm to the circulation in the subtropics. Note that the timing of the anomalies is different at 3 hPa (around 40 km) and 32 hPa (around 24 km), reflecting the downward propagation of the westerly and easterly shear zones.

The QBO-induced circulation advects relatively long-lived tracers such methane (CH_4), nitrous oxide (N_2O), water vapour (H_2O) and lower stratospheric ozone (O_3), giving rise to distinctive patterns of anomalous distributions of tracers associated both with the SAO (section 3) and the QBO (sections 4,6).

In addition to the influence on longer-lived tracer chemicals, there is also an influence on shorter-lived chemicals via their temperature dependence (section 7). This can result in substantial percentage variations from year to year e.g. in nitric acid (HNO_3), nitrogen dioxide (NO_2) and dinitrogen pentoxide (N_2O_5), associated with the QBO.

A significant inter-hemispheric asymmetry in the timing and amplitude of the subtropical anomaly in temperature and trace gas distributions is also evident. This is due to the interaction of the QBO / SAO induced circulation with the annual cycle (section 6.2).

Plumb and Bell (1982) also noted that the advective effects of the meridional circulation can account for the observed asymmetry in the descent of the equatorial QBO easterlies and westerlies. Downward advection of momentum associated with the westerly shear zone enhances the descent of the westerlies, while the upward advection of momentum associated with easterly shear inhibits the descent of easterlies.

2. Long Lived Chemical Tracers

We can learn a lot about the mass flow in the middle atmosphere from distributions of quasi-conservative chemical 'tracers'. The usefulness of a chemical as a transport tracer depends crucially on its 'chemical lifetime' i.e. the characteristic timescale for replacement or destruction by local sources or sinks compared with the 'dynamical timescale' i.e. the time for advective processes to transport the tracer (e.g. through a scale height in the vertical or from pole to equator meridionally). If the chemical lifetime is very long, the chemical will be well-mixed and of little use as a tracer. If the chemical lifetime is very short, it's distribution will be entirely determined by local photochemical processes so that if the chemical is advected it will quickly adjust to its new surroundings and there will be no 'memory' of where it came from. If, on the other hand, the chemical and dynamical timescales are similar, the distribution will be determined by both transport and chemistry. If there are suitable vertical or meridional gradients (or both) in tracer distribution, then evidence of advection by the meridional circulation will be present in the tracer distribution.

In order to examine meridional circulations associated with the SAO and QBO we use a variety of tracers depending on which height region they have a good vertical gradient. CH_4, N_2O and H_2O have been especially useful in helping to understand meridional circulations associated with the SAO. Volcanic aerosol and O_3 have been useful for diagnosing the QBO circulation.

N_2O and CH_4 both have sources in the troposphere, are slowly transported into the stratosphere where they are destroyed by photolysis or oxidation, with a chemical lifetime of the order of months (see figures 6a and 6b). Their distributions therefore decrease with height, with useful vertical gradients in the mid to upper stratosphere. On the other hand, H_2O increases with height in the stratosphere, since it's prime stratospheric source is via methane oxidation. It has useful vertical gradients in the mid to upper stratosphere and also near the tropical tropopause region, although interpretation of the latter is complicated by the temperature dependence of water vapour in this region, as it enters the stratosphere from the troposphere via tropical upwelling. Volcanic aerosol injected into the lower stratosphere after major eruptions e.g. El-Chichon and Pinatubo also has useful vertical gradients in the lower stratosphere. Finally, and importantly, there is also a very marked QBO signature in ozone, although this is complicated to interpret since there are wide variations in its chemical lifetime with height.

3. The Semi Annual Oscillation: Influence on Chemical Tracer Distributions

The time-series of equatorial zonal wind shows that there is a descending region of westerly shear in the upper stratosphere and lower mesosphere (35-60 km) in Feb – April and August – October (figure 7). This implies a region of anomalous equatorial descent propagating downward from around 60 km in February and August to around 35 km in April and October.

Early satellite observations of N_2O and CH_4 have helped in the study of the SAO influence. Figure 6 shows the solstice and equinox distributions in 1979. Around January and July, during the solstice periods, there is a single maximum in trace gas centred approximately over the equator, consistent with tropical upwelling. The maximum is slightly off the equator into the summer hemisphere, consistent with advection by the mean summer-to-winter circulation during these times. Around March-May and November, however, this distribution is replaced by a 'double peak', with two maxima at around 30°S and 30°N above about 40 km. 2-dimensional modelling experiments have demonstrated that this is due to the induced meridional circulation associated with the descending westerly shear zones of the SAO (e.g. Gray and Pyle 1987). The maximum amplitude of the double peak in trace gases is found to slightly lag the maximum in westerly shear by about a month because the trace gases take a while to respond to the anomalous circulations. Also, the amplitude of the double peak is rather smaller in November and less prolonged than in March-April. This is believed to be due to an asymmetry in strength of the westerly shear zone around October compared with March.

More recent observations in figure 8 have confirmed the double peak feature. In fact, these more recent observations have revealed a noticable QBO influence on the strength of the double peaks. In April 1993 and 1995 the double peaks are strong and well-formed but in 1994 and 1996 they are much smaller and less well-formed (Ruth et al., 1997, Randel et al. 1998). There is, of course, an expectation that the zonal wind QBO might influence the strength of the SAO westerly forcing and hence the strength and timing of the westerly shear. The waves responsible for the forcing of the SAO westerly phase propagate upwards through the equatorial lower stratosphere, which is dominated by the QBO. During the easterly phase of the QBO the westerly phase-speed waves propagate more effectively and the westerly forcing in the SAO height region is greater than during the opposite (westerly) phase of the QBO. However, figure 8 shows that the double peak structures are stronger during the *westerly* QBO phase, and not the easterly phase as one might expect. In a modelling study, Kennaugh et al (1987) showed that this is because in easterly QBO phase years the westerly shear and induced circulation associated with the SAO westerly phase is indeed stronger (as expected) but it descends through the atmosphere so quickly that the tracers do not have sufficient time in which to respond! In westerly QBO phase years the SAO-induced circulation descends more slowly and thus remains at any one level for long enough that the tracer distributions are able to respond.

4. Influence of the QBO on Aerosol Distributions

As already mentioned, major volcanoes that inject aerosol into the lower stratosphere provide useful tracers of anomalous meridional circulations in the height region of the QBO. Fig 9 shows a classic study of aerosol observations (Trepte and Hitchman 1992). The top panel shows the distribution soon after the eruption of Mount Ruiz in 1984 during a descending westerly phase of the QBO. The bottom panel shows the distribution soon after the Mount Pinatubo eruption, during a descending easterly QBO phase. The direction of the implied QBO-induced circulations are marked by arrows. The aerosol distributions mirror these extremely well, with a well-formed double peak structure during the descending west QBO phase (top panel) and evidence of enhanced ascent during the descending east QBO phase (bottom panel). Note that the double peak in this figure is at 25 km, well below the level of the SAO double peak structures (40-50 km) described in the previous section.

5. Ozone: Background

Ozone has a central role in the Earth's atmosphere. Fig. 10 shows the typical height – latitude distribution of ozone in 'parts per million by volume' (ppmv). The maximum is only of the order 10 ppmv, situated over the equator at around 10 hPa (approx. 30-35 km). The total column abundance of ozone determines the amount of radiation that can reach the surface of the Earth in the near-ultraviolet region. 'Total' or 'column' ozone is defined as the equivalent thickness of the ozone layer at standard temperature and pressure. The global mean value is approximately 3mm. Maps of column ozone are usually expressed in terms of Dobson Units (DU) where 1 DU = 10^{-5}m, so that the global mean column ozone is approximately 300 DU. Figure 11 shows the time evolution of column ozone at all latitudes throughout the year. There is an equatorial minimum of around 240 DU present at all times of the year. At high latitudes there are maxima in springtime of each hemisphere, reaching around 450 DU in the NH in April and around 380 DU in the SH in November. (Note the local minimum near the South Pole in October, coinciding with the Antarctic polar vortex. After 1985, when this plot was produced, the Antarctic Ozone Hole becomes much more evident).

Figure 12 shows results of an analysis to determine trends in NH mid-latitude ozone amounts. Percentage deviations in total column ozone averaged over the latitude band 25^{o}-60^{o}N are plotted from ground-based and satellite observations. Note the substantial inter-annual variations in these measurements, a large part of which is associated with the QBO. In order for an accurate assessment to be made of the ozone trends over the past few decades, and in order to be able to model the atmosphere sufficiently well to make accurate predictions of future ozone trends, it is essential that the variability associated with the ozone QBO is understood, accounted for and removed from these trend analysis.

The photochemical lifetime of ozone varies substantially with height in the atmosphere, as illustrated by fig 13. The lifetime is of the order of hundreds of days at 20 km but reduces rapidly with height to only half a day at 45 km. As discussed earlier, by examining variations in tracer distributions, we can learn most about advection processes in the region where the chemical lifetime is of the same order as the dynamics (months). In the case of column ozone, this is the region around 25-30 km. The major features in the time-latitude section of column ozone (fig 11) can thus be understood in terms of the mean circulation across this 25-30 km region together with a knowledge of the background distribution of ozone (fig 10). The equatorial minimum in column ozone (fig 11) at all times of the year is due to tropical upwelling in this region, bringing up air with lower ozone amounts. The two maxima in spring of each of the hemispheres (April in the NH, October in the SH) can be explained as the accumulated result of transport by the mean summer-to-winter meridional circulation, with descent throughout the winter months transporting high ozone amounts from the equatorial source region down into the lower stratosphere.

6. The Quasi Biennial Oscillation: Influence on Ozone

The QBO in column ozone is best illustrated by satellite observations e.g. from the SBUV (Solar Backscattered Ultra Violet) instruments in figure 14, which shows the latitude time-series of column ozone anomalies. The main features are an alternating equatorial anomaly of around 6-10 DU (approx. 4% of the background total column amount), a phase change in the subtropics and a subtropical / midlatitude anomaly of opposite sign of around the same magnitude.

6.1 Equatorial Ozone QBO

The equatorial column ozone anomaly is closely associated with the equatorial zonal wind QBO and figure 14 shows clearly the irregular timing of the equatorial QBO, with anomalies that sometimes last only 9-12 months (e.g. 1982, 1983) and sometimes 12-18 months (e.g. 1989/90). Note, therefore, that the equatorial ozone QBO signal, like the zonal wind QBO, is not synchronized with the annual cycle.

Fig 15 shows the time-series of SBUV equatorial column ozone anomaly together with a reference QBO wind time-series (Randel and Wu 1996). There is excellent correspondence between the observed ozone anomaly and the reference wind series. Positive (negative) anomalies are present when the zonal winds in the lower stratosphere are westerly (easterly). To understand this relationship between zonal wind and ozone QBO signal, we consider the westerly QBO phase as an example. The time of the maximum westerly vertical wind shear at a particular level corresponds to the time of the warmest phase of the equatorial temperature QBO and hence to the time of maximum relative descent. (Remember that this does mean that there is actual descent, since the zonal mean circulation is always upwards at the equator in the lower stratosphere; relative descent simply means that this upwelling is weaker than the average). This anomalous descent occurs in the height region where the background ozone amounts increase with height (see fig 10). Thus, anomalous descent through the 25-30 km height region produces an anomalous increase in column ozone. Above about 30 km the ozone lifetime is relatively short (figure 13) and ozone is replaced by chemical production relatively quickly. Fig 16 shows a schematic of this process. The maximum total column ozone anomaly is the accumulated response to the descent of the westerly shear zone and will therefore occur when the column has been displaced farthest downward into the lower stratosphere. This will occur after the descent of the westerly shear to the lowermost stratosphere i.e. around the time of the maximum westerly anomaly at 20-25 km.

Although the above mechanism accounts for a large component of the QBO in column ozone, there are nevertheless a number of additional factors that influence the column anomaly. Figure 17 shows the time height cross section of the QBO ozone density anomaly (DU km^{-1}). This can be used to visually determine the contribution from each height range to the total column anomaly (which is simply a sum in the vertical of the ozone density anomaly). Below about 28 km i.e. where the ozone lifetime is of order months, ozone is dynamically controlled and shows a gradual downward propagation of the anomaly with time, corresponding to the downward propagation of the shear zones with time. However, there is also a small contribution from above 28 km, where the chemical lifetime of ozone is shorter and is controlled by QBO changes in its photochemical sources and sinks (see section 7 for further details). The anomalies at the two levels are approximately a quarter cycle out of phase. There is therefore a small contribution to the column from above 28 km that also influences the timing of the total column anomaly.

As mentioned earlier, changes in ozone distributions in the lower stratosphere have radiative implications and, in particular, have a direct effect on short-wave heating. The effect of including the coupling between the ozone QBO anomalies and heating rates in computer models of the QBO tends to reduce the heating rate that would otherwise be calculated from a given temperature anomaly in the lower stratosphere. This is therefore an additional factor that needs to be taken into account when trying to understand the phase relationship between the QBO signals in ozone and zonal wind.

6.2 Subtropical and Mid-latitude Ozone QBO

A QBO signal in column ozone in the subtropics that extends to middle and high latitudes is clearly evident in fig 14. There is a 180^o phase change at around 15^o in each hemisphere with the higher-latitude anomaly extending to at least 60^o but with its maximum at approximately 30^o- 40^o latitude. The subtropical anomaly corresponds broadly to the return arm of the local equatorial QBO circulation, with ascent (descent) in the subtropics associated with westerly (easterly) equatorial shear.

However, there are several significant departures from the expected behaviour. Firstly, the induced equatorial QBO circulation is confined to low latitudes and hence cannot explain the signal poleward of about 30^o. Secondly, the timing and the amplitude of the subtropical anomalies are not symmetric about the equator; the subtropical minima and maxima are approximately 6 months apart and coincide with the local late winter / spring. This latter feature is highlighted in fig 18 which shows a regression fit of Total Ozone Mapping Spectrometer (TOMS) column ozone amounts to the 30 hPa Singapore winds (Randel and Cobb 1994). On average, the subtropical regression anomalies reach a maximum in March and August in the NH and SH respectively. There is therefore a change in the period of the anomaly as one moves to higher latitudes.

Jones et al. (1998) used a 2-d model to show that this hemispheric asymmetry in the amplitude and timing of the subtropical and higher latitude ozone QBO is caused by an asymmetry in the QBO-induced meridional circulation. Rather than being symmetric about the equator, as figure 2 implies, their modelled circulation was strongest in the winter hemisphere. This is confirmed by figure 19 that shows a cross-section of the QBO temperature anomaly and (residual mean) circulation in February 1994 derived from assimilated meteorological analyses (Randel et al., 1999). There is induced ascent coinciding with the minimum temperature anomaly at 25 km but a descending return arm of the circulation only in the NH subtropics and not the SH subtropics. Similarly, the temperature anomaly is highly symmetric.

Jones et al. (1998) noted that because the QBO zonal wind jets are symmetric about the equator, the horizontal gradient $\partial\tilde{u}/\partial y$ is asymmetric (where $\tilde{u}$ is the QBO-induced component of the zonal wind. Additionally, under solstice conditions, the background (QBO-independent) zonal wind gradient $\partial\bar{u}/\partial y$ is also highly asymmetric. Hence, sdvection terms, particularly $\bar{v}(\partial\bar{u}/\partial y)$ and $\tilde{v}(\partial\bar{u}/\partial y)$ introduced strong hemispheric asymmetry into the QBO-induced meridional circulation.

Figure 14 shows that occasionally there is a 'missed' subtropical anomaly, for example, in 1981, 1986 and 1991 in the NH and in 1993 in the SH. These missed anomalies are probably due to the timing of the equatorial QBO relative to the annual cycle. The formation of a significant winter subtropical anomaly requires not only a strong QBO-induced circulation but also a strong background (summer-to-winter) horizontal advection to help strengthen the winter side of the circulation. These conditions need to last for a month or two to allow the ozone distribution to respond to the induced circulation. If either of these requirements is not present for a sufficiently long time, the subtropical anomaly is unlikely to form in that year. Similarly, if the timing and duration of the equatorial wind QBO is such that it persists in the same phase for two successive winters, then anomalies of the same sign will occur in successive winters in the subtropics of that hemisphere. The latter is evident in the SH in 1983-1984 and 1988-89.

The mechanism for the poleward extension of the subtropical ozone QBO signal to mid-latitudes is not well understood. It is likely to involve an interaction between planetary waves and the equatorial QBO. The modulation of planetary wave forcing by the equatorial wind QBO results in a stronger large-scale (summer-to-winter) circulation in easterly phase years. Stronger downwelling in the winter midlatitudes will produce a positive (negative) column ozone anomaly in easterly (westerly) years, as observed (Tung and Yang, 1994). On the other hand, the extension of the ozone anomalies to middle and higher latitudes may be due to mixing processes associated with planetary scale waves.

At midlatitudes, therefore, a number of factors and feedback processes may contribute to the ozone anomaly.

There is also an indication of a QBO influence in the winter polar regions. The polar ozone QBO is approximately in phase with the midlatitude ozone QBO and is seasonally synchronised in the same way, with maximum amplitude in springtime (Garcia and Solomon 1987, Randel and Cobb, 1994). Observational evidence for the polar ozone QBO is statistically less significant, partly due to the high level of interannual variability in the springtime vortex. It is possible that there may be a feedback loop between the modulation of the extratropical temperature by the QBO (due to a QBO in planetary wave transport), the formation of polar stratospheric clouds (which is highly temperature dependent) and hence with the underlying chemical destruction that gives rise to the ozone hole (Mancini et al. 1991, Butchart and Austin, 1996).

7. The Quasi Biennial Oscillation: Influence on Other Trace Gases

Model studies of the QBO that include a treatment of chemical processes in the stratosphere in addition to the dynamical and radiative processes predict a strong QBO in many of the trace gases that have a relatively short chemical lifetime. This includes e.g. members of the nitrogen family and chlorine family. A short chemical lifetime means that the trace gas distribution will not show any response to advection by the mean circulation (since it will very quickly re-establish photochemical equilibrium to its new surroundings). However, it may still show a response to the QBO in temperature or to a QBO signal in any other trace gas that influences its chemistry. These model predictions have subsequently been confirmed in some of the trace species for which there are adequately long time-series of measurements.

7.1 The Nitrogen family

Figure 20 shows the latitude time-section of the QBO signal in a variety of trace gases at 22 km, taken from an idealised 2-dimensional model study (Gray and Chipperfield 1990). Although the lifetime of, for example, NO_2 is relatively short, it may be considered as part of a 'family' of nitrogen-containing trace gases, general referred to as NOy, the odd nitrogen family. While there may be chemical interactions and hence relatively short timescale variations in concentration of the individual members of the family, the sum of the individual members

$NOy = NO_2 + NO + HNO_3 + 2N_2O_5 + HO_2NO_2 + ClONO_2$

has a relatively long chemical timescale. The distribution of NOy in the stratosphere increases with height in the lower stratosphere, so the QBO signal in NOy is similar to the column ozone QBO anomaly. It has a negative (positive) anomaly in equatorial latitudes during the easterly (westerly) phase of the zonal wind QBO, a phase change at around 20° and a subtropical anomaly of opposite sign, with an asymmetry in the amplitude of the subtropical anomaly. There is a peak-to-peak variation of approximately 25% at the equator. This variation is much larger than the 10% percentage variation in

N_2O at this level and reflects the steeper vertical gradients in NOy compared with N_2O. As already mentioned, the chemical lifetime of NO_2 is relatively short and the QBO signal is therefore not a direct result of the QBO-induced circulation. Instead, it is a result of the temperature QBO through the temperature dependence of the following reaction:

$NO + O_3 \rightarrow NO_2 + O_2$

A positive temperature anomaly at the equator, associated with a westerly shear zone, results in the NO:NO_2 partitioning being shifted in favour of NO2, resulting in a positive NO_2 anomaly. The converse is true in the case of easterly shear. The resulting percentage variation at this level is 30-40 %.

The modelled percentage variation in N_2O_5 is extremely large, of the order of 60-70 %. Again, this is due to the temperature dependence of the key chemical reaction that influences the abundance of N_2O_5. At present, there are no measurements of N_2O_5 with which to confirm this prediction.

The 'chemically-controlled' ozone QBO anomaly above about 28 km in figure 17 (as opposed to the 'transport-controlled' anomaly below 28 km) can be explained by changes in the photochemical sources and sinks of ozone, primarily via transport-induced variations of NOy (Chipperfield et al. 1994, Jones et al. 1998).

7.2 Water vapour

Figure 21 shows the distribution of water vapour in the stratosphere (ppmv) in January 1993 and January 1994 measured by satellite. Unlike the troposphere, the stratosphere is very dry, the main source being via methane oxidation. For this reason, water vapour mixing ratios increase with height (remember that methane decreases with height). Note the minimum value situated at the tropical tropopause and a single-peaked structure centred over the equatorial latitudes that is almost a mirror-image of the methane distribution. This single-peak structure is consistent with the mean tropical upwelling advecting relatively dry air from the region of the minimum at the tropical tropopause higher into the stratosphere. There is some indication of the influence by the induced QBO-circulation, indicated by the arrows.

Figure 22 shows the time-height section of the QBO anomalies in H_2O over the equator for the period 1992-99. The QBO anomaly ascends slowly with time, in contrast to the slow descent of the ozone QBO. This upward propagation is a reflection of the dynamics affecting the equatorial tropopause minimum. There is a well-defined annual signature in the tropopause water vapour minimum, closely tied to the annual temperature variation. This annual minimum in H_2O is advected upwards by the background tropical upwelling. (This is sometimes called the 'tape recorder' effect, since the annual 'imprint' of cold temperatures is imposed on the water vapour distribution and this signal is then advected upwards and away from the tropopause region). Figure 21(a) shows that the minimum is centred around 40 hPa in January 1993 and has a rather flat, pancake shape. In January 1994 however, it is slightly higher up and has a more rounded, circular shape (figure 21(b)). One possible mechanism for this QBO signal in tropical H_2O is a QBO-modulation of the tropical ascent rate, which is expected to be stronger in an easterly QBO wind shear zone than in the westerly shear zone. However, this does not appear to be the whole explanation, since there are some discrepancies between the observed behaviour of water vapour and methane. Another possibility is the QBO in tropopause temperatures since the water vapour abundance at tropopause level is highly dependent on the temperature as it enters the lower stratosphere through the tropopause region. More research is required to fully understand this QBO signal.

Figure 21 also indicates a fairly substantial QBO influence on the H_2O distribution in the subtropics and mid latitudes. For example there is a so-called 'staircase' effect in January 1994 (figure 21(a)) with isolines of H_2O nearly vertical at points B and C, but nearly horizontal at point D (Dunkerton and O'Sullivan, 1996). This is an example of the competing influences of vertical advection by the mean circulation that will tend to steepen the isolines versus the influence of planetary-scale mixing processes that will tend to flatten the isoline gradients (Gray, 2000).

References:

- Butchart, N. and J. Austin, On the relationship between the quasi biennial oscillation, total chlorine and the severity of the Antarctic ozone hole. *Q.J.Roy. Meteorol.* Soc., 122, 183-217, 1996.
- Chipperfield, M.P., L. J. Gray. J.S. Kinnersley, and J. Zawodny, A two dimensional model study of the QBO signal in SAGE II NO_2 and O_3, Geophys. Res. Lett., 21, 589-592, 1994.
- Dunkerton, T.J. and D.J. O'Sullivan, Mixing zone in the tropical stratosphere above 10 mbar, *Geophys. Res. Lett.*, 23, 2497-2500, 1996.
- Garcia, R. R., and S. Solomon, A possible relationship between interannual variability in Antarctic ozone and the quasi-biennial oscillation, *Geophys. Res. Lett.*, 14, 848-851, 1987.
- Gray, L.J., A model study of the influence of the quasi biennial oscillation on trace gas distributions in the middle and upper stratosphere. *J. Geophys. Res.*, 105, 4539-4551, 2000.
- Gray, L.J. and M.P. Chipperfield, On the interannual variability of trace gases in the middle atmosphere, *Geophys. Res. Lett.*, 17, 933-936, 1990.
- Gray, L.J. and J.A. Pyle, The semi annual oscillation and equatorial tracer distributions, *Q.J.R. Meteorol. Soc.*, 112, 387-407, 1986.
- Jones, D. B. A., H. R. Schneider, and M.B. McElroy, Effects of the quasi-biennial oscillation on the zonally averaged transport of tracers. *J. Geophys. Res.* 103, 11,235-11,249. 1998.
- Kennaugh, R., S. Ruth, and L.J. Gray, Modeling quasi-biennial variability in the semiannual double peak, *J. Geophys. Res.*, 102, 16,169-16,187, 1997.
- Mancini, E., G. Visconti, G. Pitari and M. Verdecchia, an estimate of the Antarctic ozone modulation by the QBO, *Geophys. Res. Lett.*, 18, 175-178, 1991.
- Plumb, R.A. and R.C. Bell, Equatorial waves in steady zonal shear flow, *Q.J. Roy. Meteorol. Soc.*, 108, 313-334, 1982a.

- Plumb, R.A. and R.C. Bell, A model of the quasi biennial oscillation on an equatorial beta plan, *Q.J. Roy. Meteorol. Soc.*, 108, 335-352, 1982b.
- Randel, W. J. and J.B. Cobb, Coherent variations of monthly mean column ozone and lower stratospheric temperature, *J. Geophys. Res.,* 99, 5433-5447, 1994. and Cobb 1994
- Randel, W.J., and F. Wu, Isolation of the ozone QBO in SAGE II data by singular decomposition, *J. Atmos. Sc.,* 53, 2546-2559, 1996.
- Randel, W.J., F. Wu, J.M. Rusell III, A. Roche and J. Waters, Seasonal cycles and QBO variations in stratospheric CH4 and H2O observed in UARS HALOE data. *J. Atmos. Sci.*, 55, 163-185, 1998.
- Randel, W.J.F. Wu, R. Swinbank, J. Nash, and A. O'Neill, Global QBO circulation derived from UKMO stratospheric analyses, *J. Atmos. Sci.,* 56, 457-474, 1999.
- Ruth , S., R. Kennaugh, L.J. Gray, and J.M. Russell III, Seasonal semiannual and interannual variability seen in measurements of methane made by the UARS Halogen Occultation Experiment, *J. Geophys. Res.,* 102, 16189-16,199, 1997.
- Trepte , C.R., and M.H. Hitchman, Tropical Stratospheric circulation deduced from satellite aerosol data, *Nature,* 355, 626-628. 1992.
- Tung, K., and H. Yang, Global QBO in circulation and ozone, part I, Re-examination of observational evidence, *J. Atmos. Sci.,* 51,2699-2707, 1994.

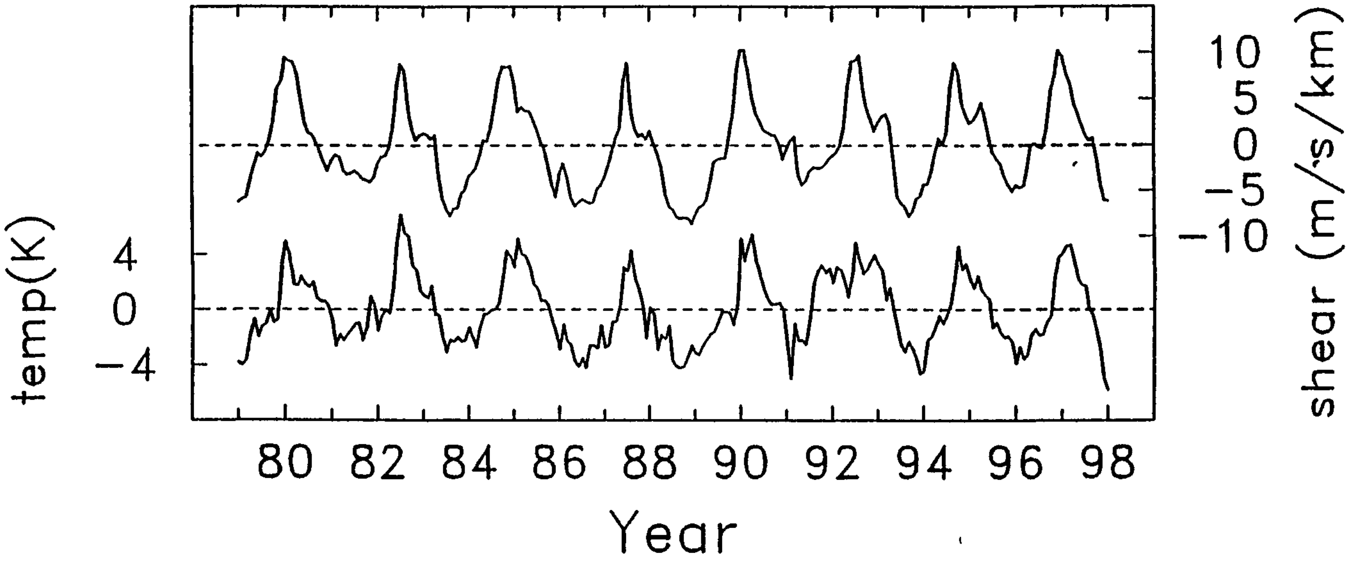

Equatorial temperature anomalies associated with the QBO in the 30- to 50-hPa layer (bot curve) and vertical wind shear (top curve)

Figure 1

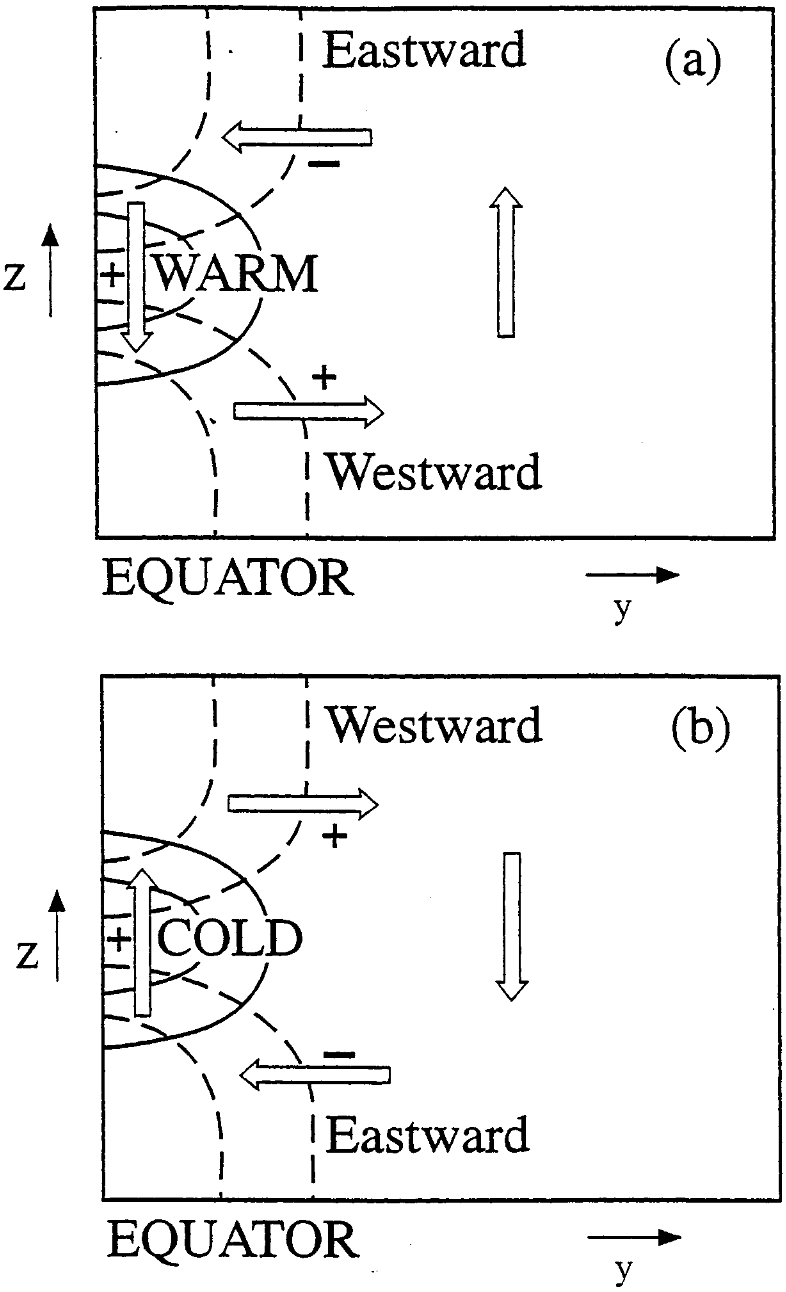

[redacted]. Schematic latitude-height sections showing the mean meridional circulation associated with the equatorial temperature anomaly of the QBO. Solid contours show temperature anomaly isotherms, and dashed contours are zonal wind isopleths. Plus and minus signs designate signs of zonal wind accelerations driven by the mean meridional circulation. (a) Westerly shear zone. (b) Easterly shear zone. After *Plumb and Bell* [1982b]. Printed with permission from the Royal Meteorological Society.

figure 2.

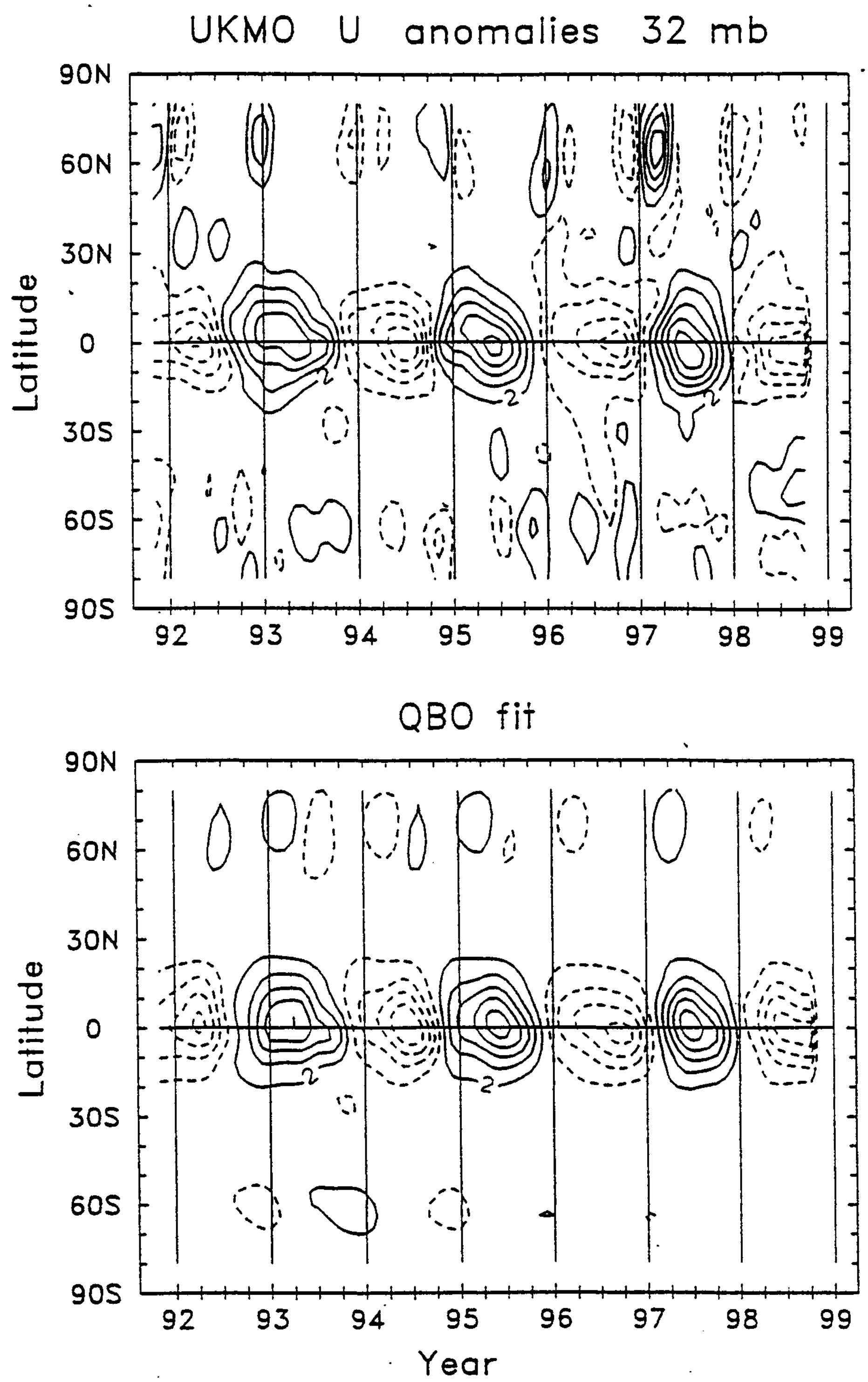

FIG. 6. Latitude–time sections of UKMO zonal wind anomalies a 32 mb. Top panel shows the full anomalies, and bottom panel is th statistical QBO fit. Contours are ±2, 6, 10, · · · m s^{-1}.

figure 3

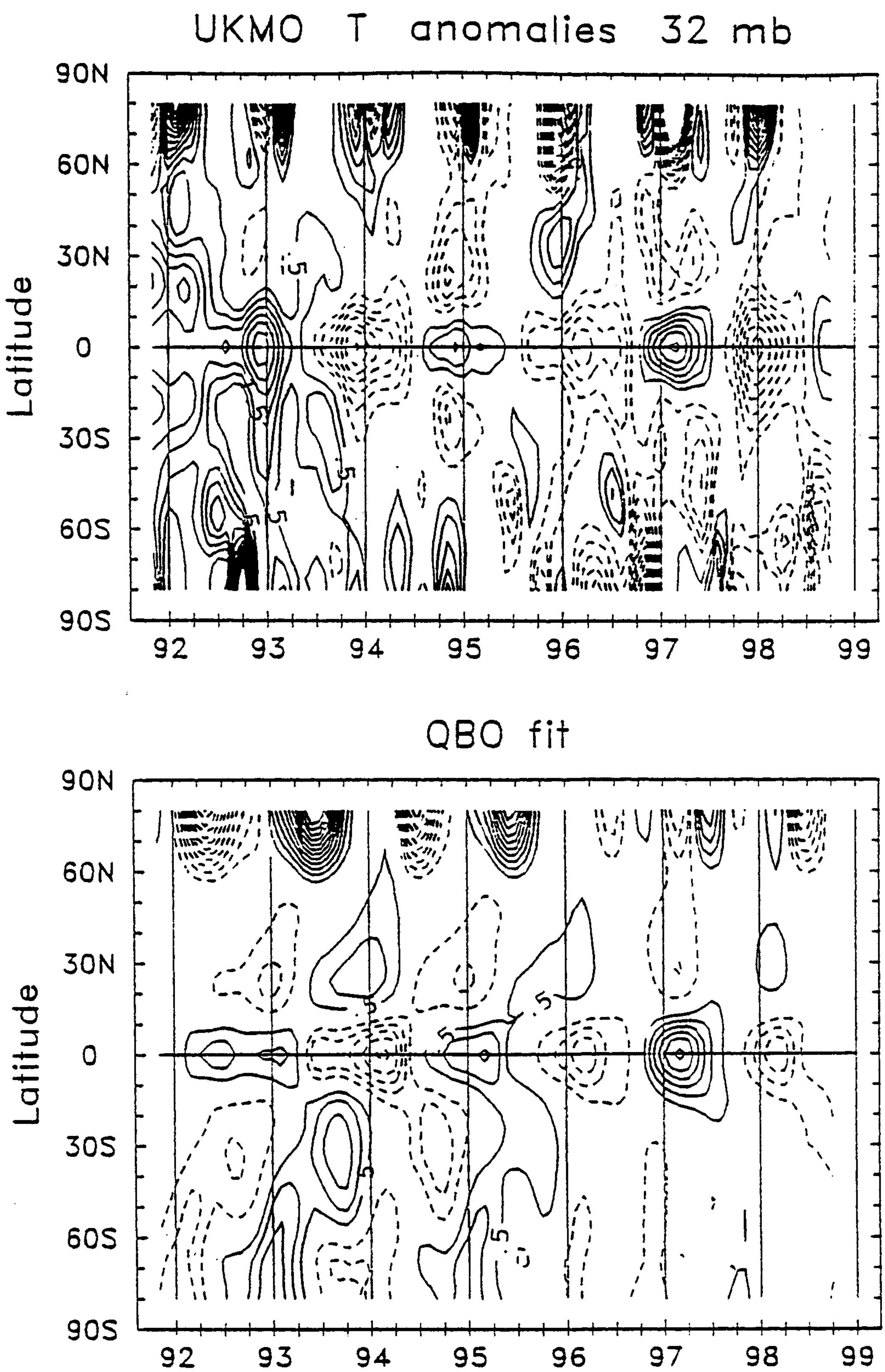

FIG. 10. Latitude-time sections of UKMO temperature anomalies at 32 mb. Shown are the full anomalies (top), the QBO statistical fit Contours are ±0.5, 1.0, 1.5, $\cdots$ K.

figure 4.

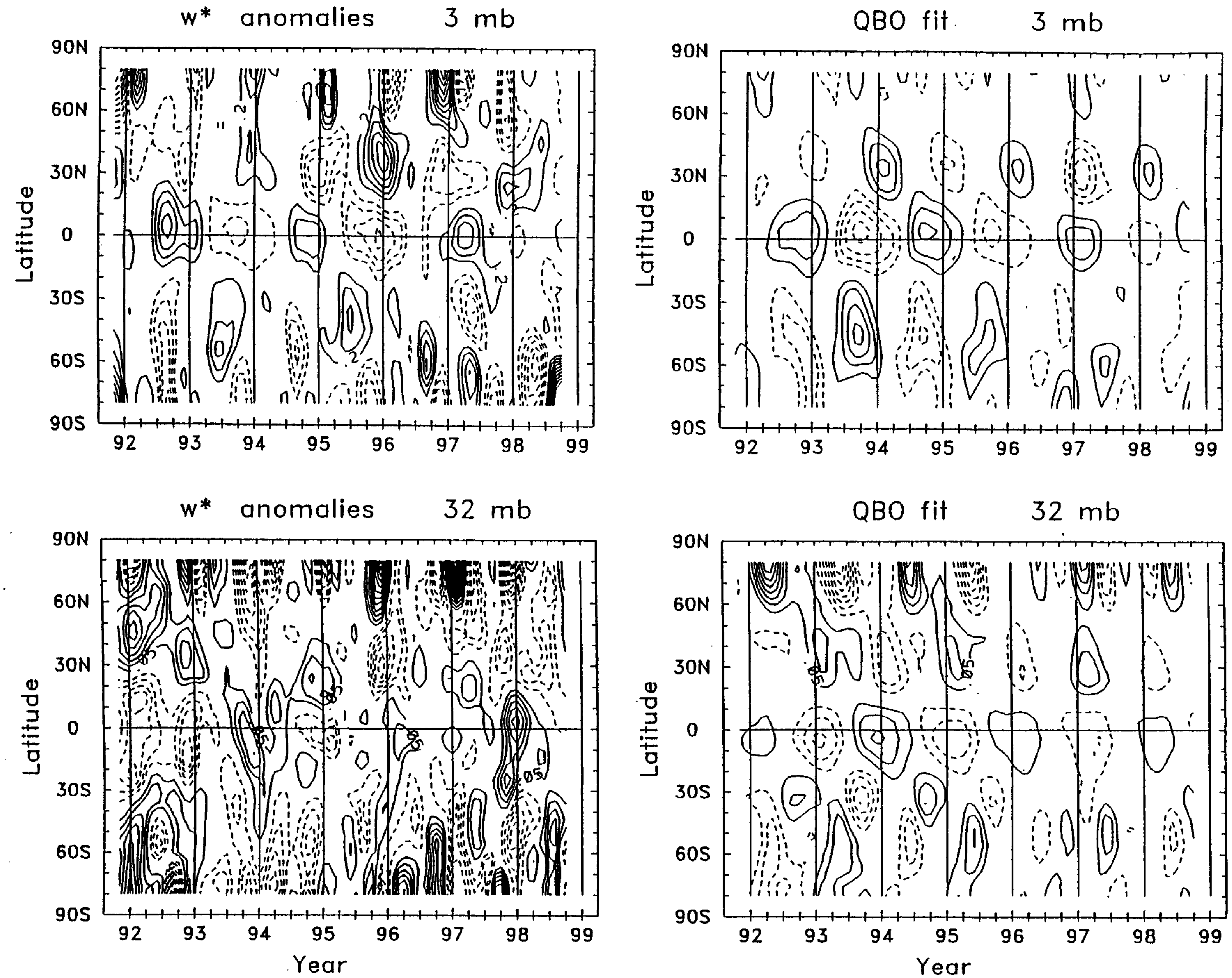

Figure 5.

FIG. 17. Latitude–time sections of residual mean vertical velocity ($\overline{w^*}$) interannual anomalies at 3.2 mb (top) and 32 mb (bottom). (Left) the full anomalies and (right) the QBO statistical fit. Contour interval is 2.0 (top) and 0.05 km/month (bottom), with zero contours omitted.

figure 6(a)

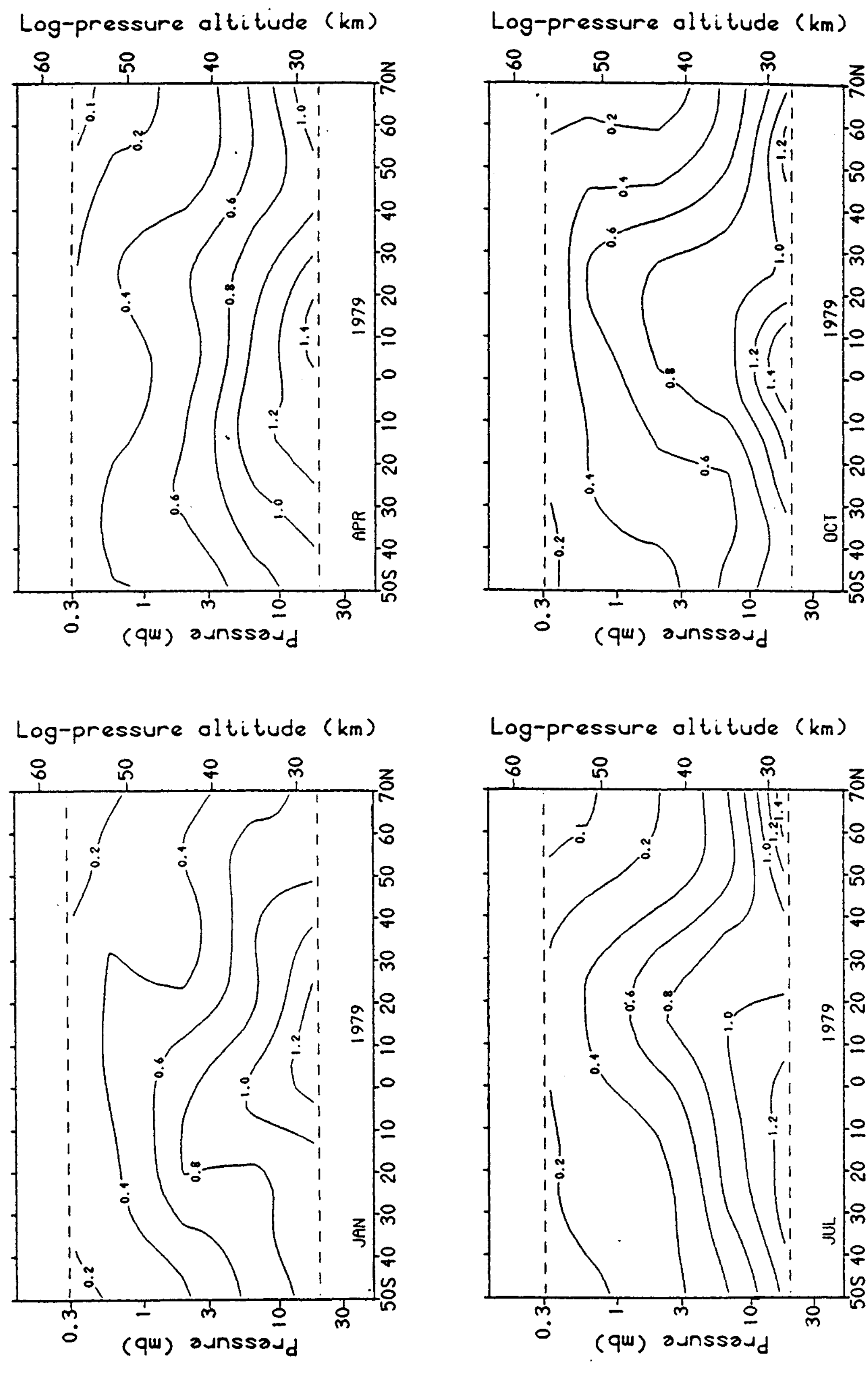
Log-pressure altitude (km)
Pressure (mb)
APR 1979
OCT 1979
JAN 1979
JUL 1979
50S 40 30 20 10 0 10 20 30 40 50 60 70N

(a)

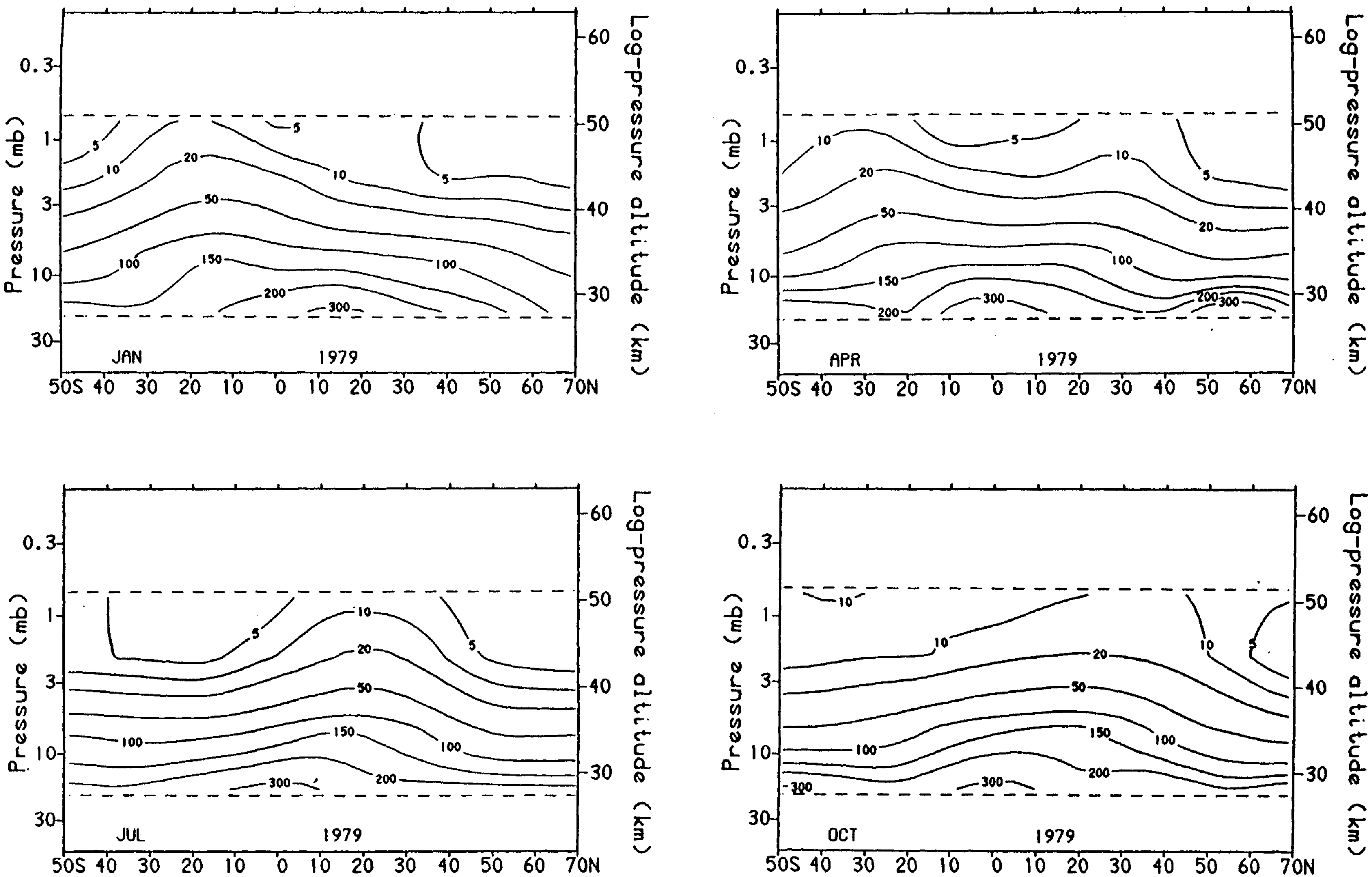

(b)

~~Fig. 9.3.~~ Monthly mean cross sections of (a) CH_4 (ppmv) and (b) N_2O (ppbv) from measurements by the *Nimbus* 7 SAMS experiment during 1979. [After Jones and Pyle (1984).]

figure 6(b)

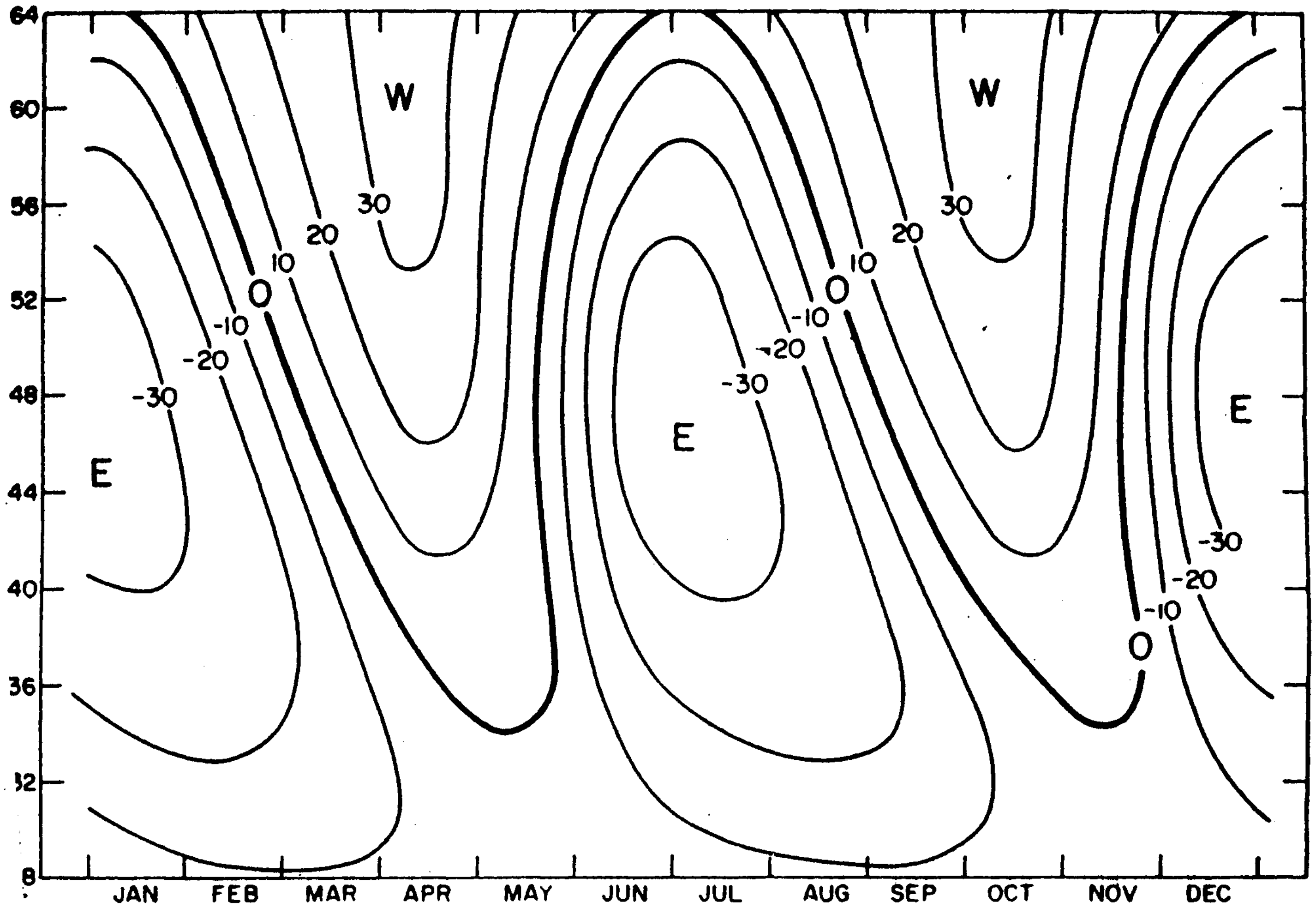

e 2. Time–height cross-section at the equator showing the estimated semi-annual mean zonal wind oscillation ($m\,s^{-1}$). (After Reed 1966)

figure 7

HALOE = Halogen Occultation Expt on board UARS (Upper Atmosphere Research Satellite)

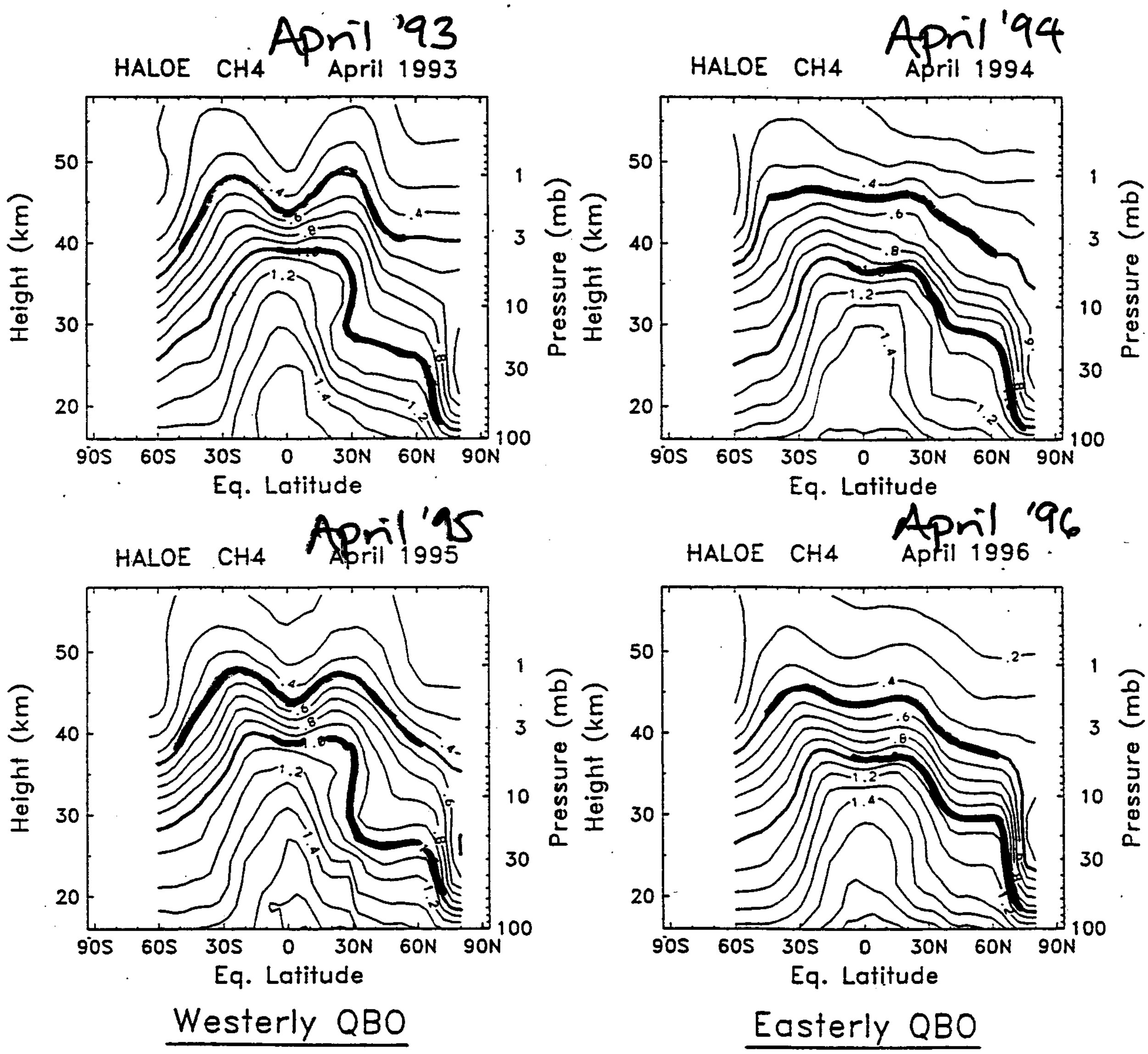

figure 8

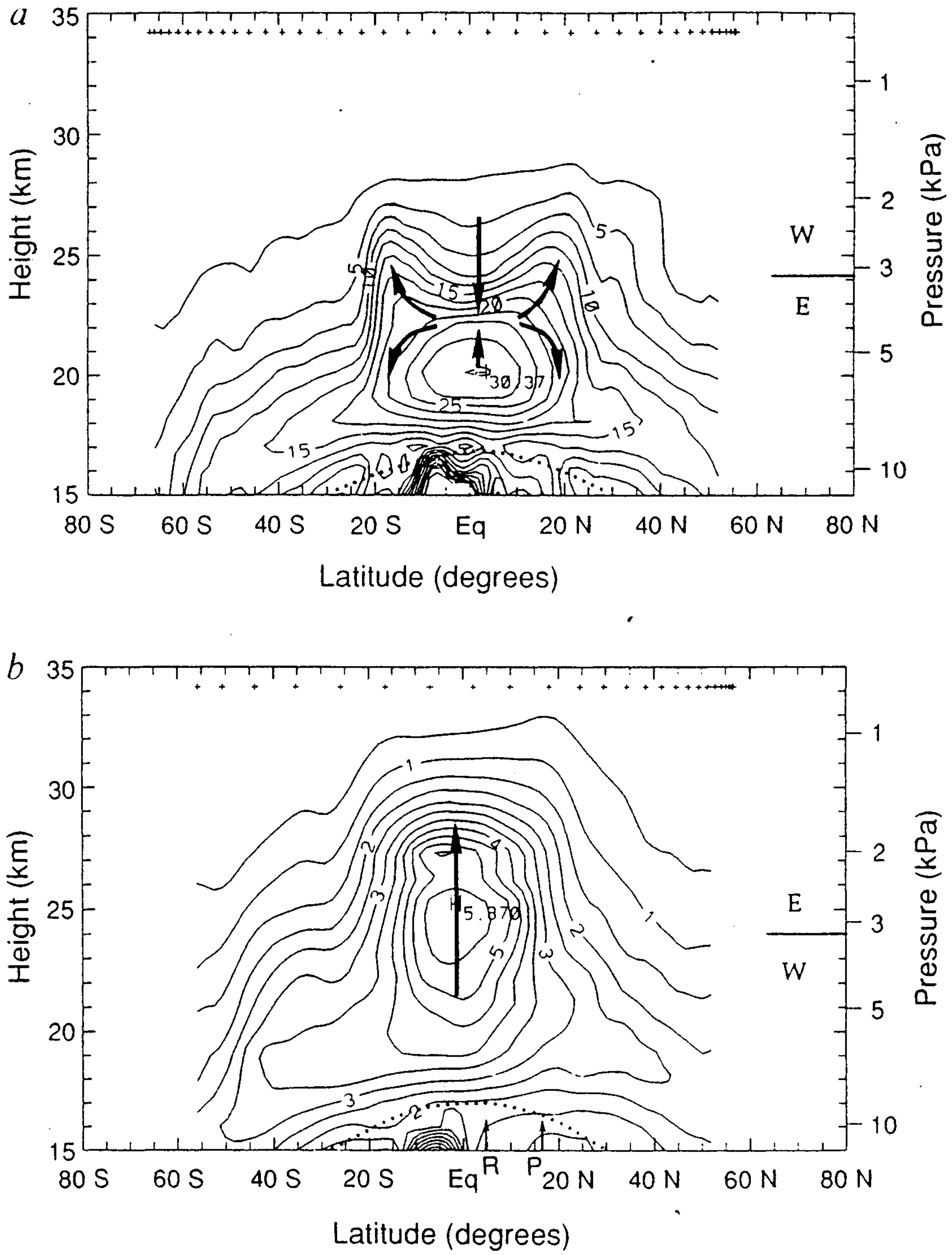

Figure 26. Latitude-height cross sections of observed aerosol extinction ratio for two 40-day periods representative of the two phases of the QBO. (a) Westerly shear phase centered on November 11, 1984 (contour interval is 2.5). (b) Easterly shear phase centered on October 4, 1988 (contour interval is 0.5). From *Trepte and Hitchman* [1992]. Reprinted with permission from *Nature*.

figure 9.

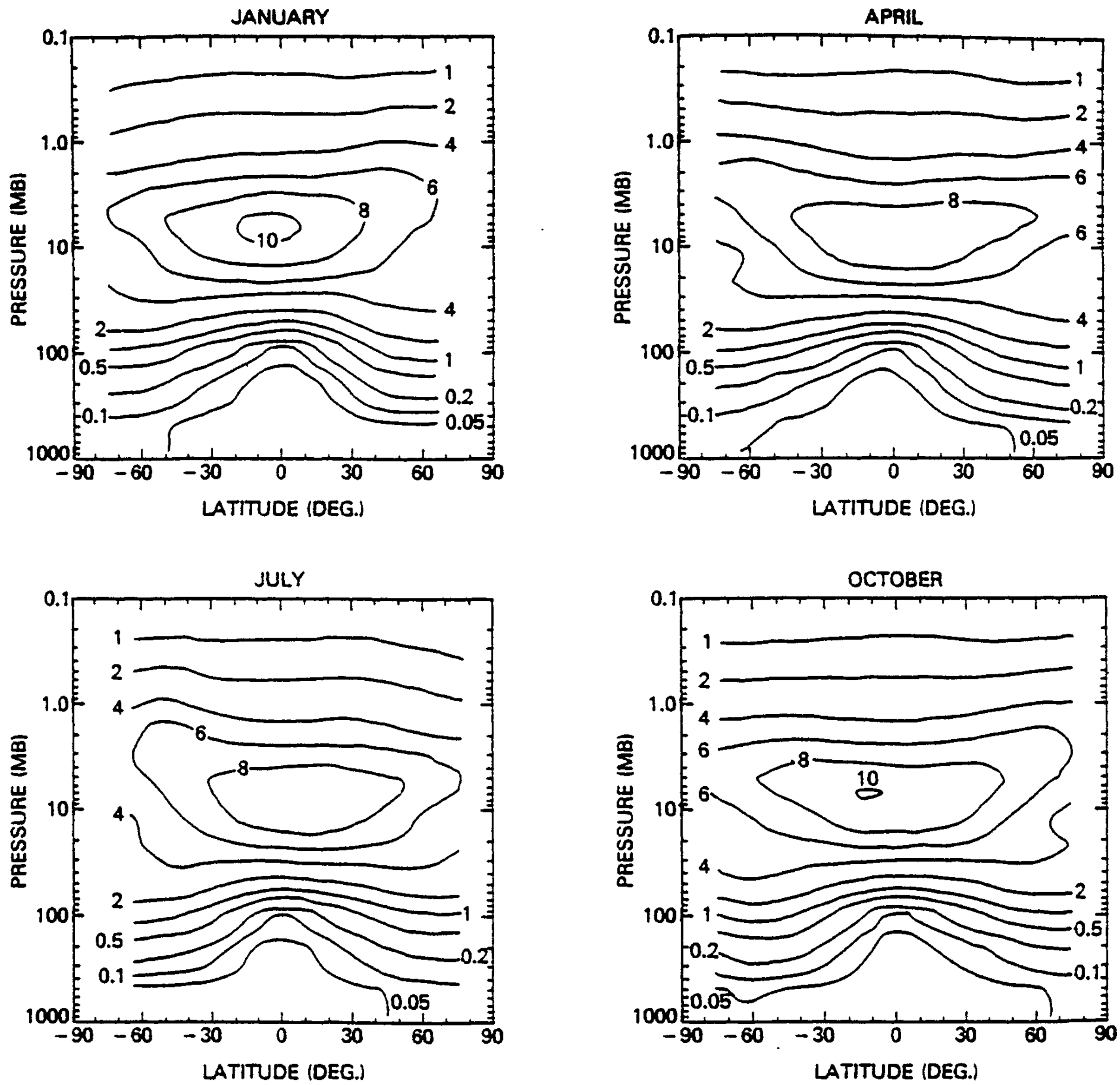

Fig. 10.4. Latitude-height sections of the ozone mixing ratio (ppmv) for January, April, July, and October 1979, as observed by the *Nimbus* 7 SBUV experiment. [After McPeters *et al.* (1984).]

figure 10.

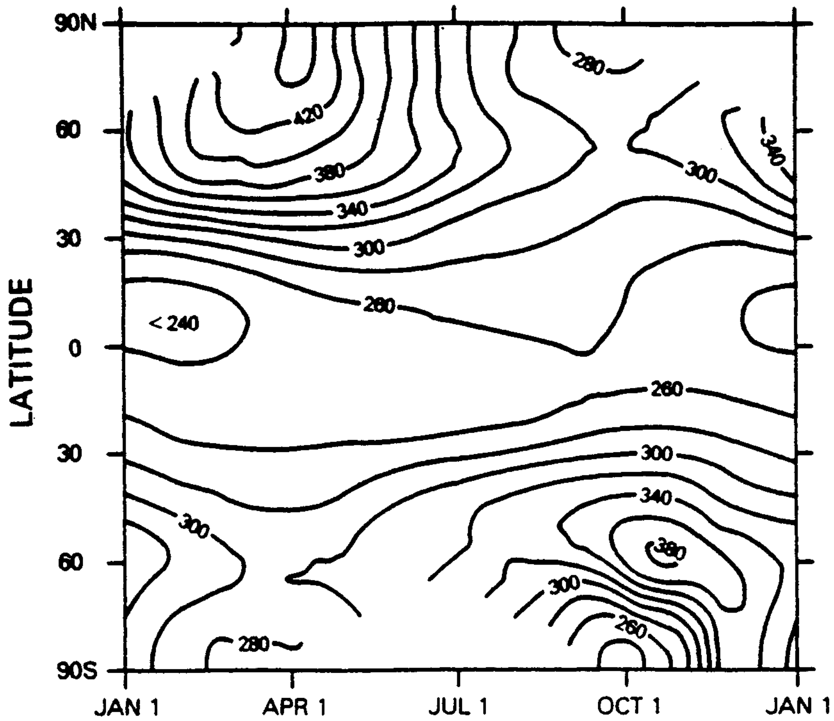

Fig. 10.2. Time-latitude section showing the seasonal variation of total ozone (Dobson units) based on TOMS data. Note the springtime maxima near 90°N and 60°S and the minimum near 90°S. [After Bowman and Krueger (1985).]

figure 11

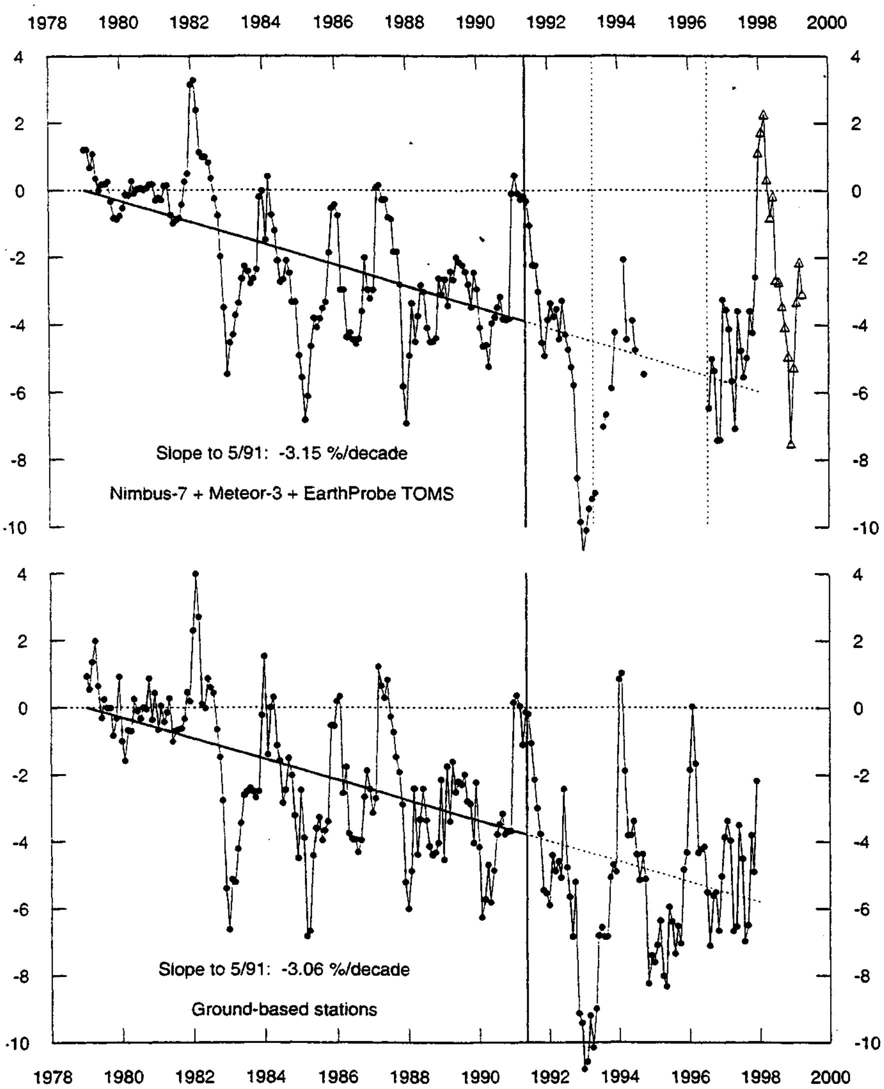

~~Figure 1.8~~

Deviations in total ozone, area weighted over 25°–60°N. A seasonal trend model (not including the effects of the solar cycle or the quasi-biennial oscillation) was fitted to the ozone data over the period from January 1979 to May 1991. The upper panel shows the TOMS record (1/79-4/99) and the lower panel shows a ground-based series constructed from average ozone at stations in 5° latitude bands (1/79–12/97). Trend models are fit independently to the two data sets. The solid straight line represents the least squares fit to the deviations up to May 1991 and is extended as a dotted line through December 1997. (The TOMS record is updated from WMO (1999) courtesy of L. Bishop, Allied Signal.)

figure 12

Photochemical Lifetime of Ozone

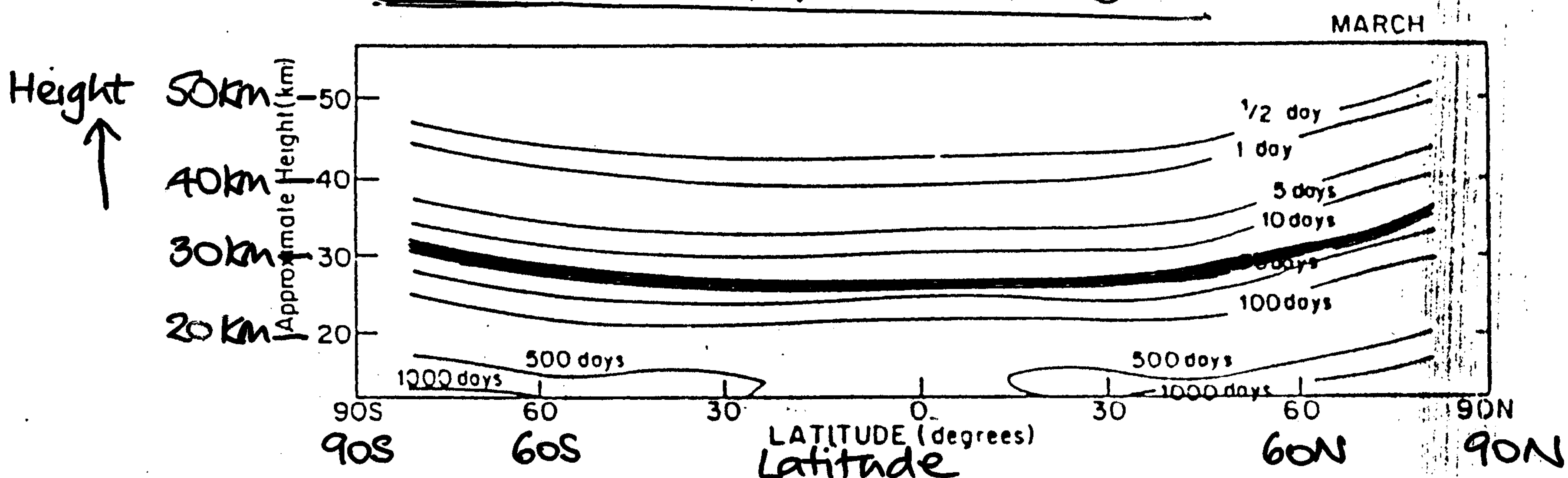

FIG. 6. Latitude-height section of the photochemical lifetime of odd oxygen in the model for the month of March. The shaded area indicates the approximate position of the transition region, that is, the region in which the photochemical lifetime is of the same order as the time scale for meridional transport (see text for a further discussion of the definition of the transition region).

figure 13

equatorial lower stratosphere. Similarly, the rele-
it quantities in March of yrs 4, 6 and 11 were av-

of that cycle of the QBO. In the following these statistics will be referred to as Marcl phase) and March (westerly phase), respec

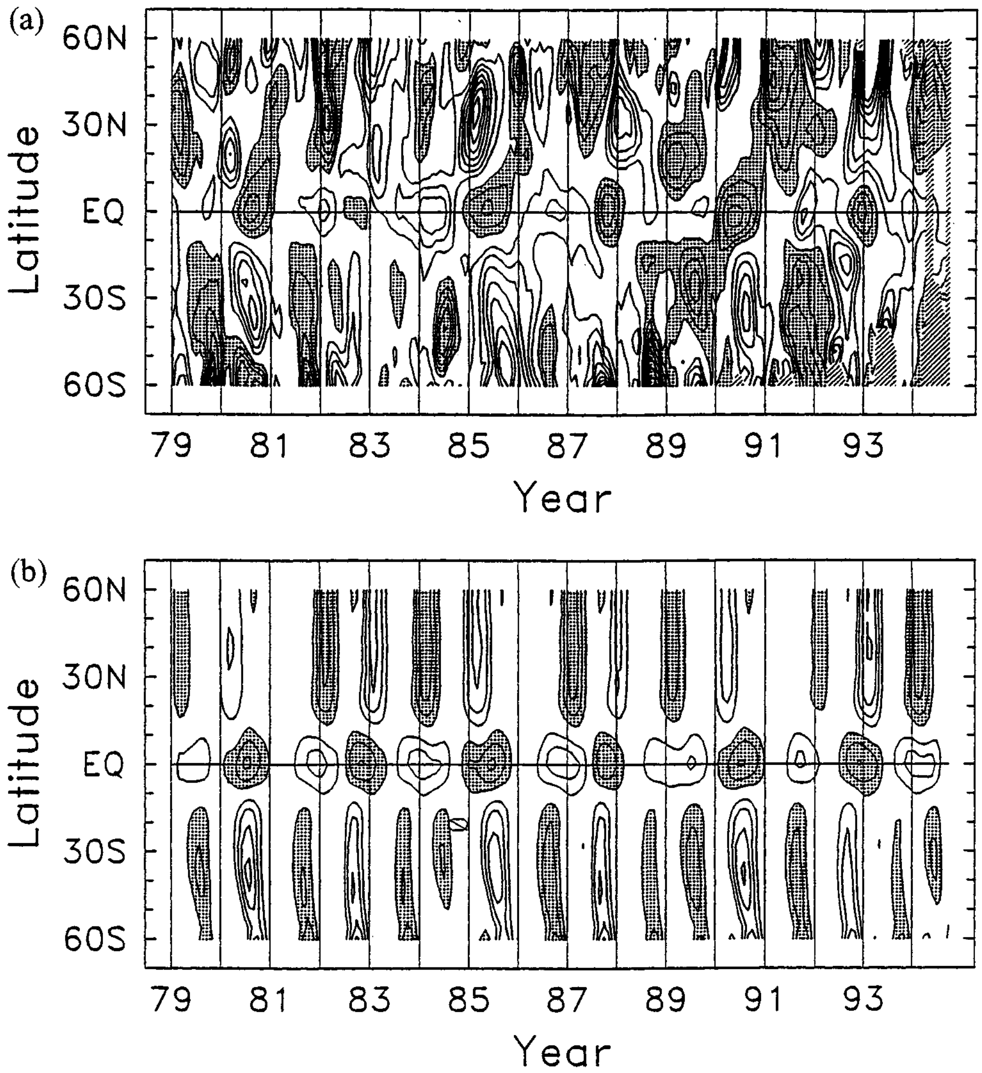

Figure 21. Latitude-time sections of column ozone anomalies from combined SBUV-SBUV/2 data: (a) full anomalies defined as deseasonalized and detrended over 1979–1994, and (b) the QBO component derived by seasonally varying regression analysis. Data in all panels were multiplied by cos (latitude) to account for area weighting. Contour interval is 3 DU, with 0 contours omitted and positive values shaded. Diagonal hatching denotes unreliable data. Vertical lines denote January of each year. Reprinted from *Randel and Wu* [1996] with permission from the American Meteorological Society.

figure 14.

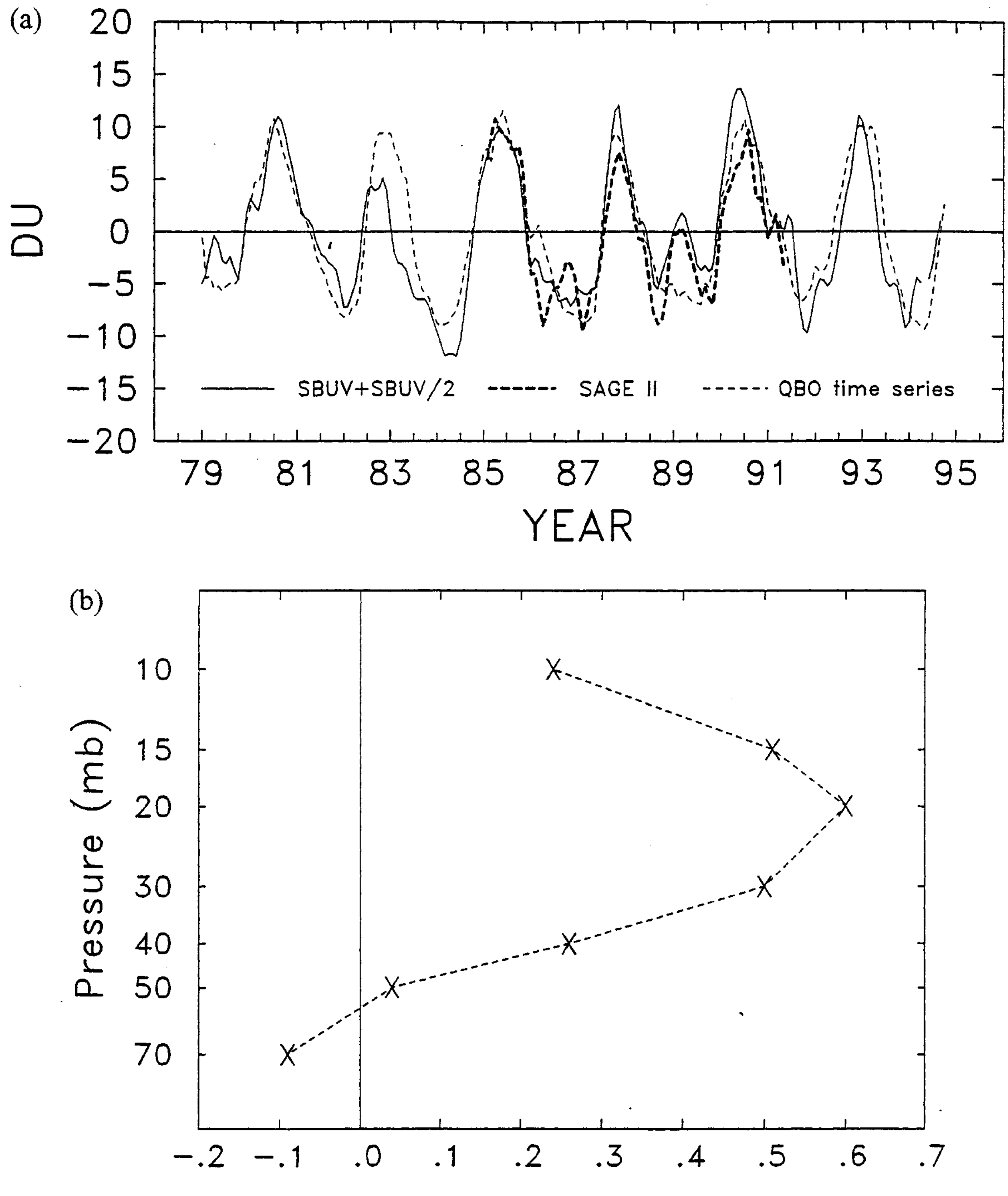

Figure 20. (a) Time series of equatorial ozone anomaly in Dobson units (DU, solid line) from solar backscattered ultraviolet (SBUV) and SBUV/2 together with a reference QBO wind time series (dotted curve) compiled by multiplying the observed winds at Singapore by the weighting profile shown in Figure 20b. Reprinted from *Randel and Wu* [1996] with permission from the American Meteorological Society.

figure 15.

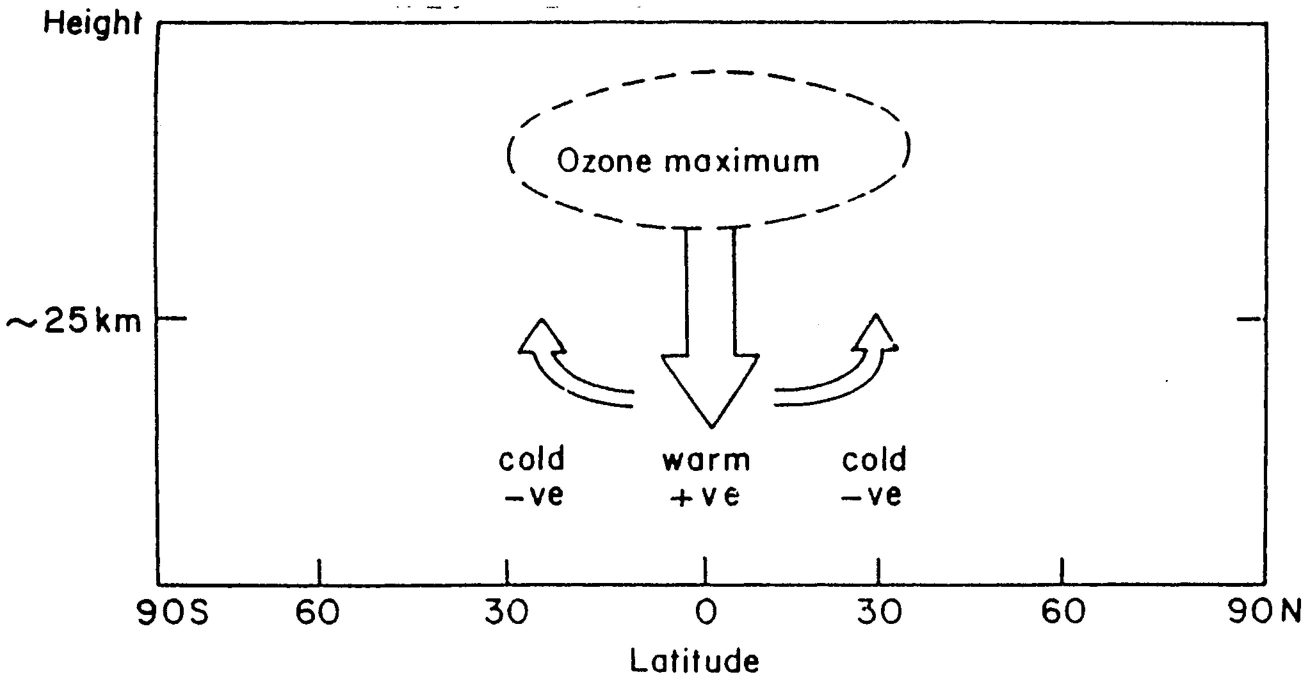

~~Fig. 2.~~ A schematic diagram showing the induced meridional circulation associated with a westerly phase of the QBO. The positive and negative signs indicate the expected column ozone anomaly.

figure 16.

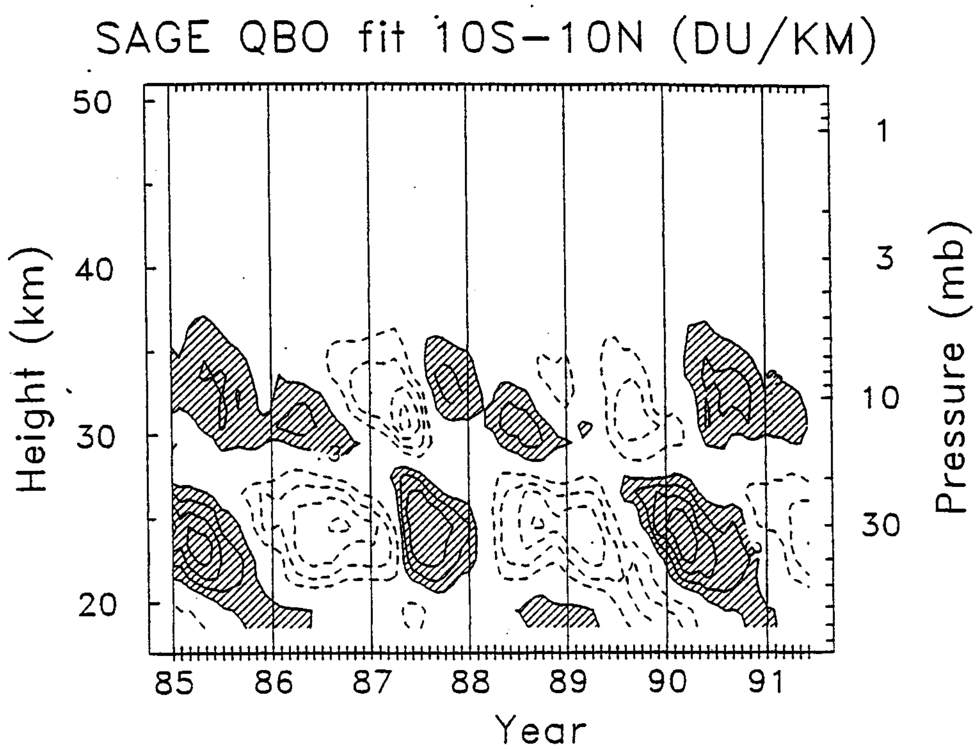

Figure 22. Height-time series of interannual anomalies in ozone density (DU km^{-1}) derived using a regression analysis to isolate the QBO variation. Contour intervals are 0.3 DU km^{-1}, with 0 contours omitted and positive values shaded. Reprinted from *Randel and Wu* [1996] with permission from the American Meteorological Society.

figure 17.

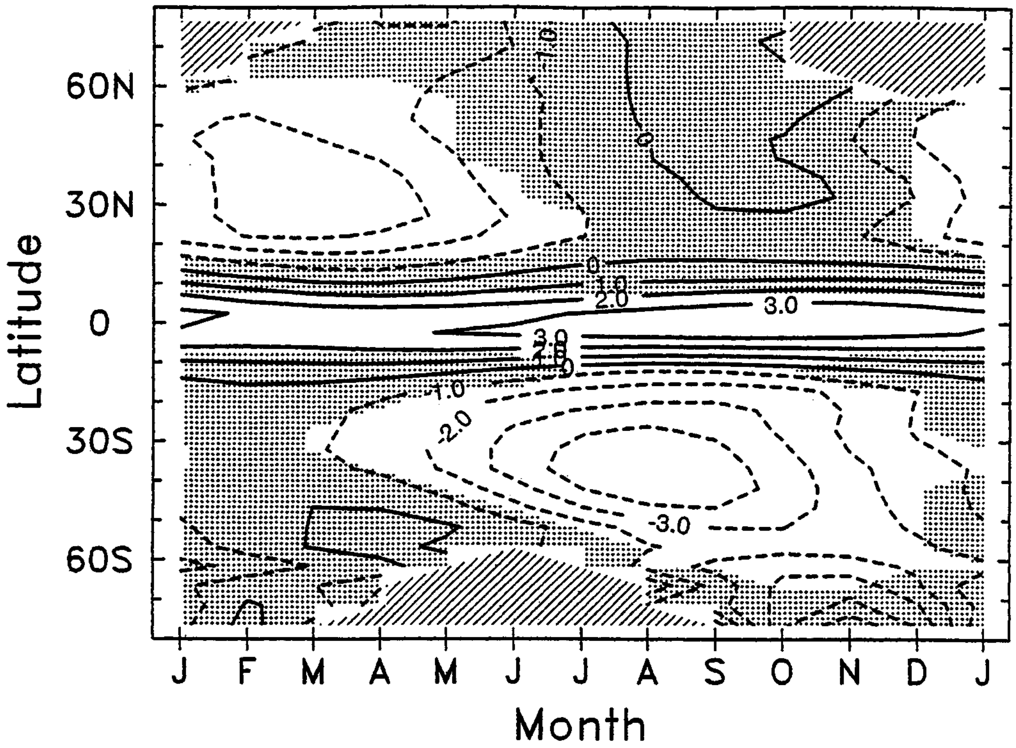

Figure 23. Latitude-time section of QBO-associated regression fit of zonal-mean Total Ozone Mapping Spectrometer (TOMS) column ozone (DU) to the 30-hPa Singapore winds for the period 1979–1994. Shading denotes regions where the statistical fits are not different from zero at the 2σ level. Hatched regions denote the polar night, where no ozone data are available. Updated from *Randel and Cobb* [1994].

figure 18

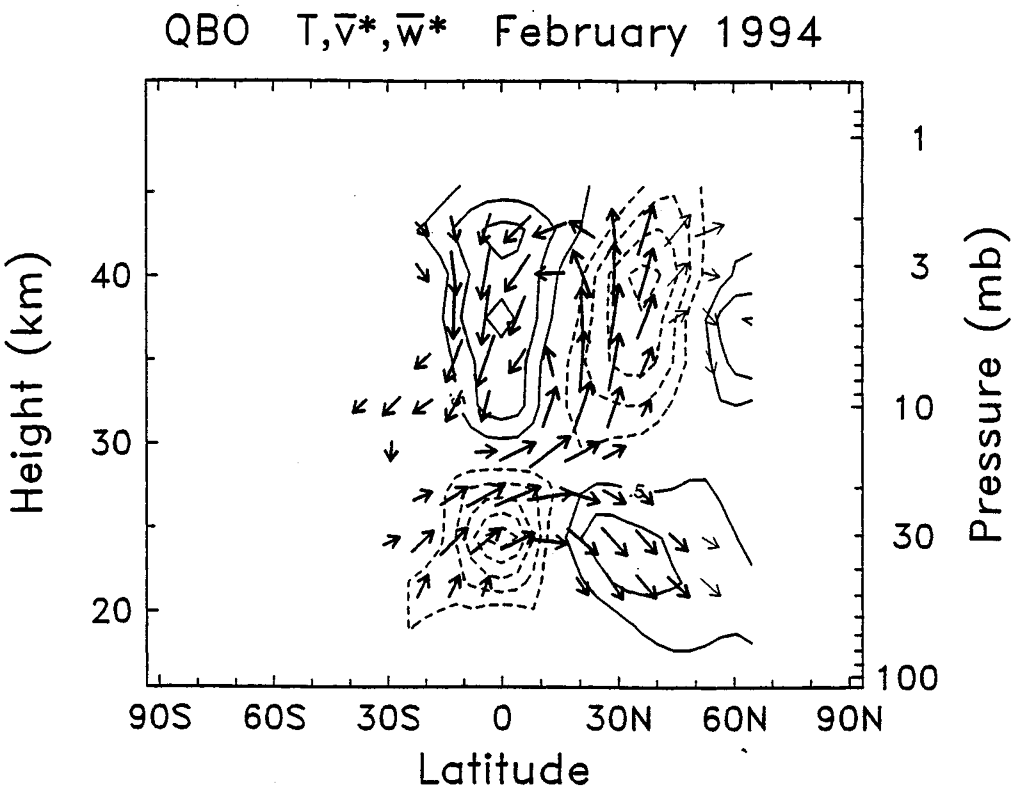

Figure 5. Cross sections of QBO anomalies in February 1994. Temperature anomalies are contoured (±0.5, 1.0, 1.5 K, etc., with negative anomalies denoted by dashed contours), and components of the residual mean circulation ($\bar{v}^*$, $\bar{w}^*$) are as vectors (scaled by an arbitrary function of altitude). Reprinted from *Randel et al.* [1999] with permission from the American Meteorological Society.

figure 19

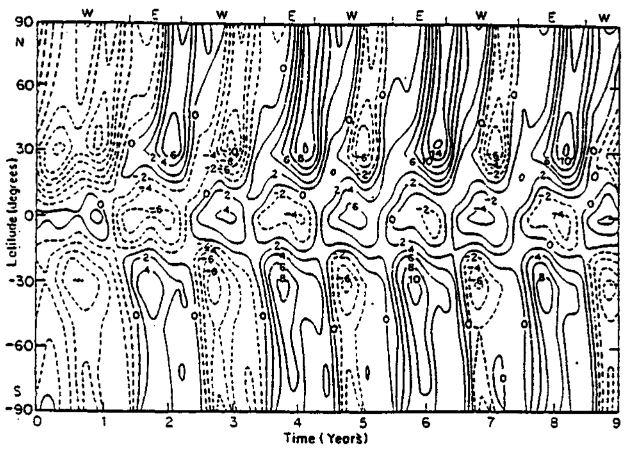

~~Fig. 1.~~ Latitude time-series of the modelled column ozone anomaly (Dobson Units). Contour interval 2 DU. Dashed lines denote negative values. The direction of the equatorial zonal winds at approximately 50 mb is indicated at the top of the figure.

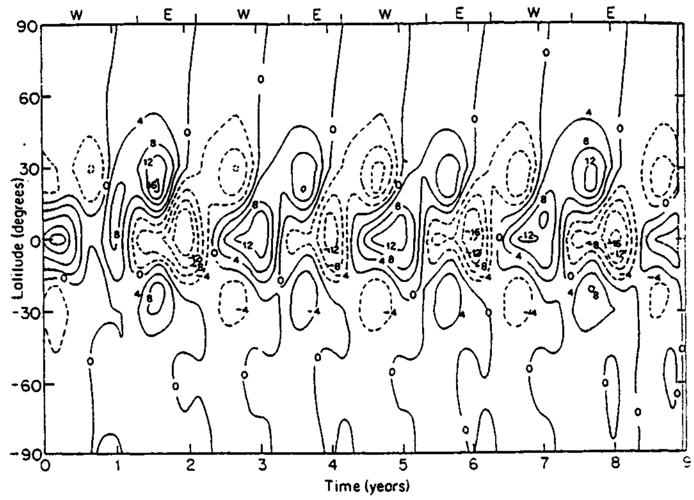

~~Fig. 4.~~ As figure 3 but for total odd nitrogen (NO + NO_2 + HNO_3 + 2 x N_2O_5 + HO_2NO_2 + $ClONO_2$). Contour interval 3%.

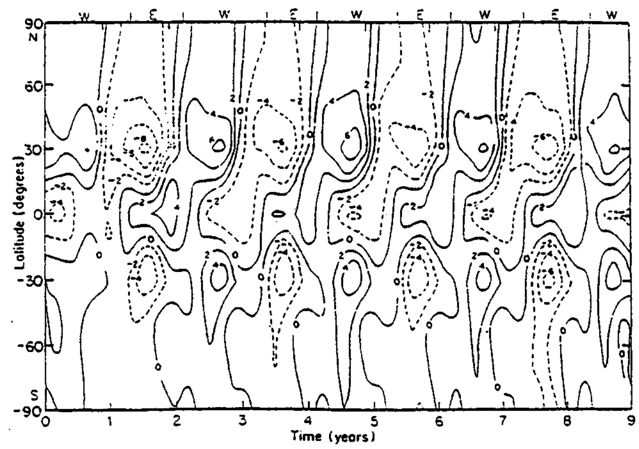

~~Fig. 3.~~ Latitude time-series of the modelled QBO anomaly in N_2O mixing ratio at 22 km expressed as a percentage of the ambient N_2O at that level. Contour interval 2 %.

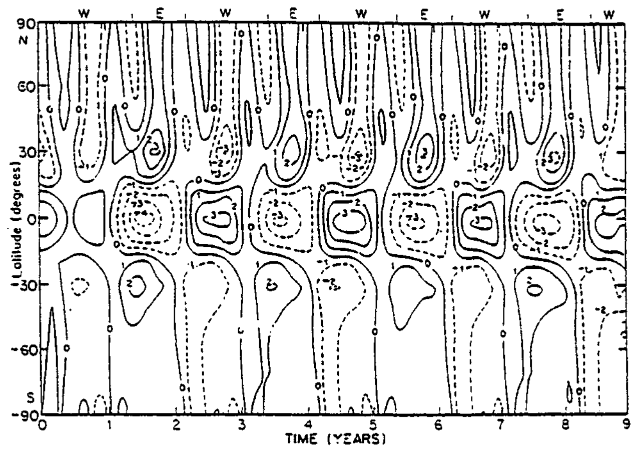

~~Fig. 6.~~ Latitude time-series of the modelled QBO anomaly in temperature in degrees Kelvin. Contour interval is 1K.

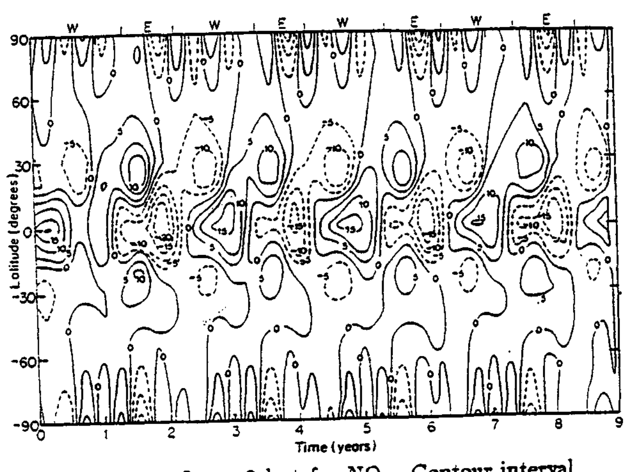

~~Fig. 7.~~ As figure 3 but for NO_2. Contour interval 4%.

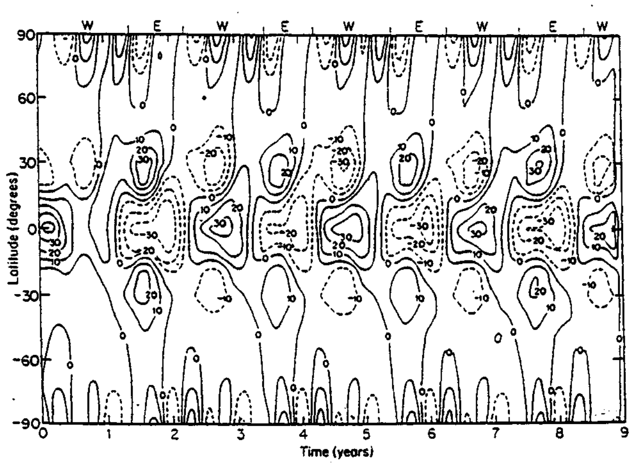

~~Fig. 8.~~ As figure 3 but for N_2O_5. Contour interval 8%.

figure 20.

HALOE (Halogen Occultation Expt): UARS (Upper Atmosphere Research Satellite)

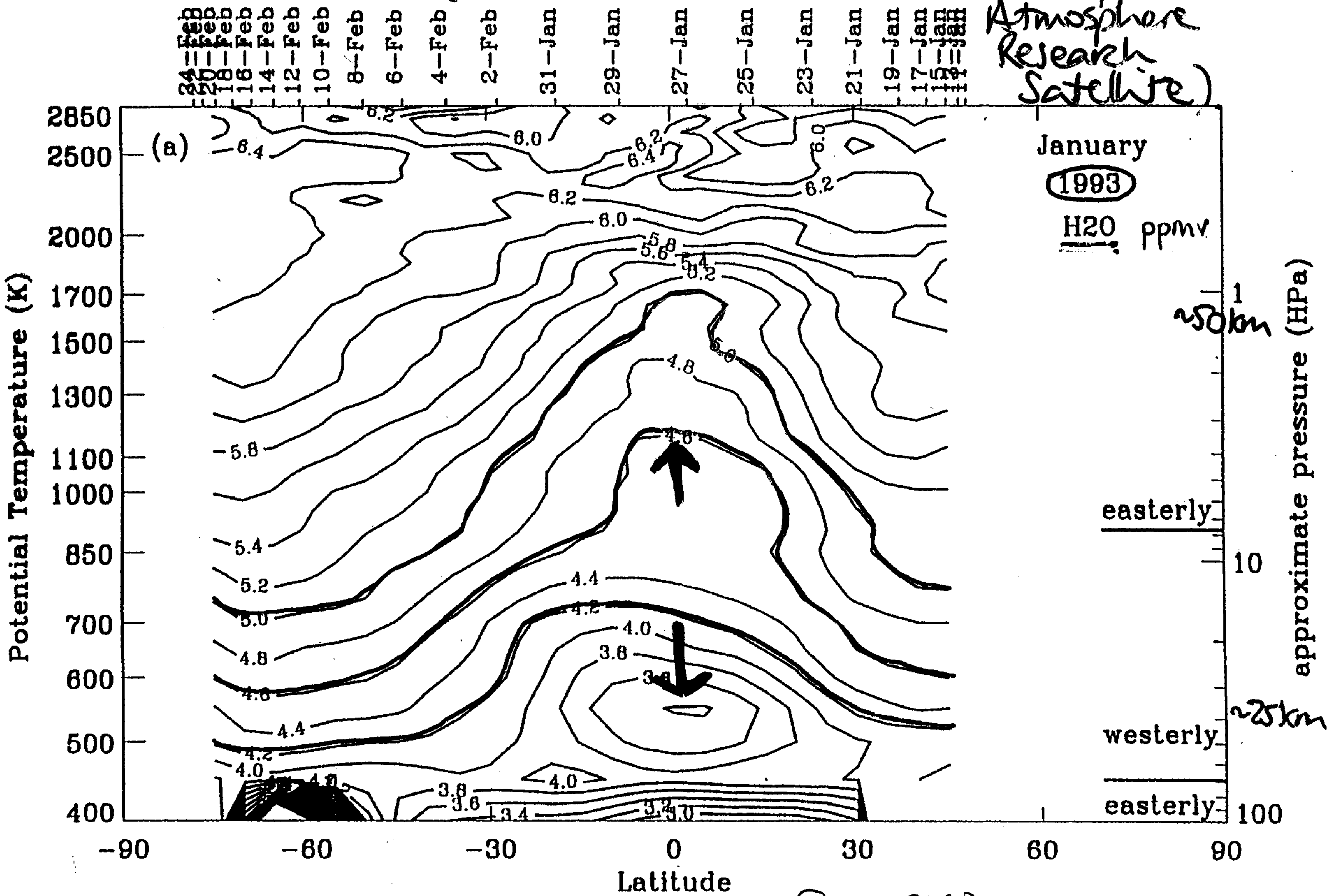

figure 21(a)

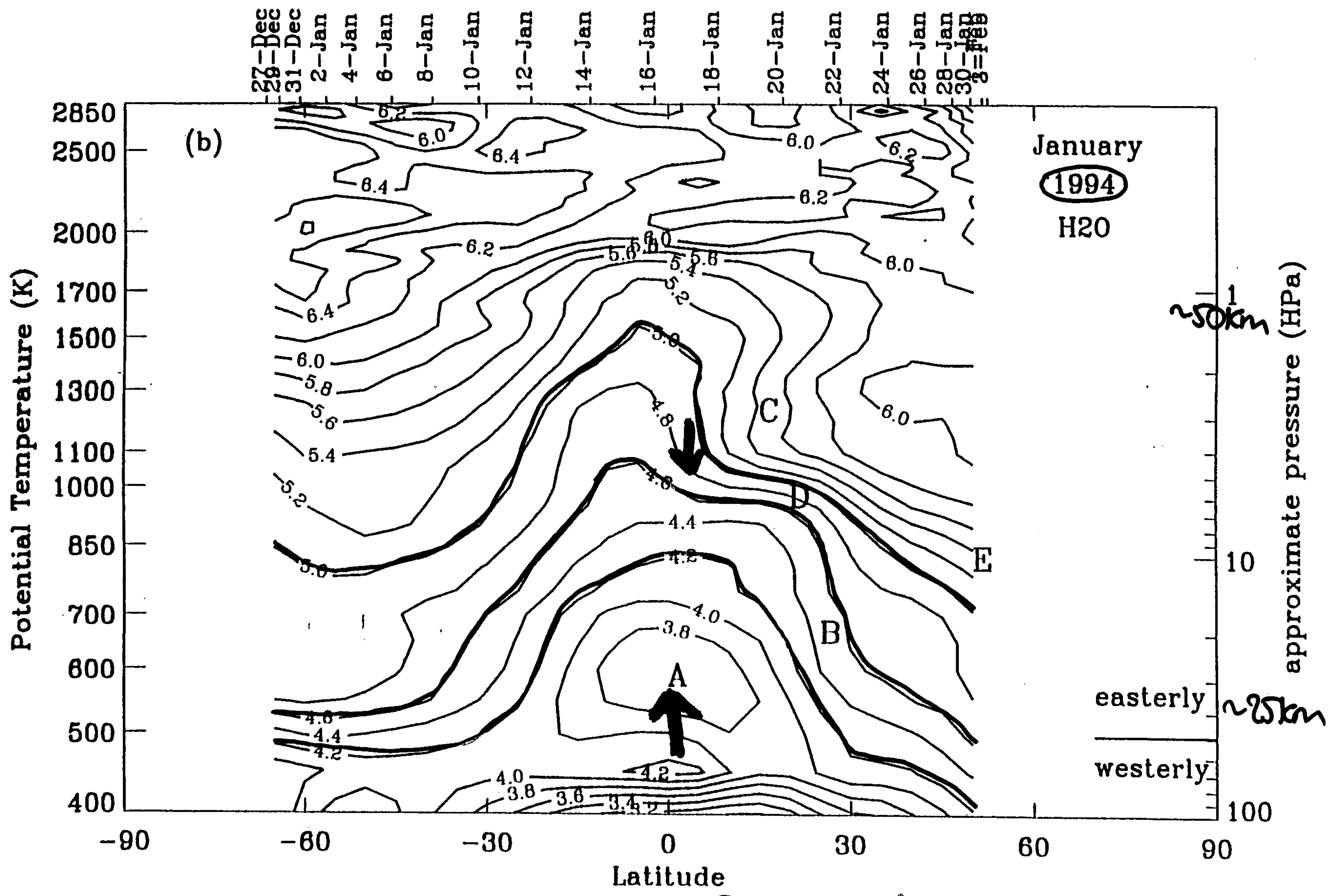

(b)
January
1994
H2O
Potential Temperature (K)
Latitude
approximate pressure (HPa)
easterly
westerly
~50km
~25km
A
B
C
D
E

figure 21(b)

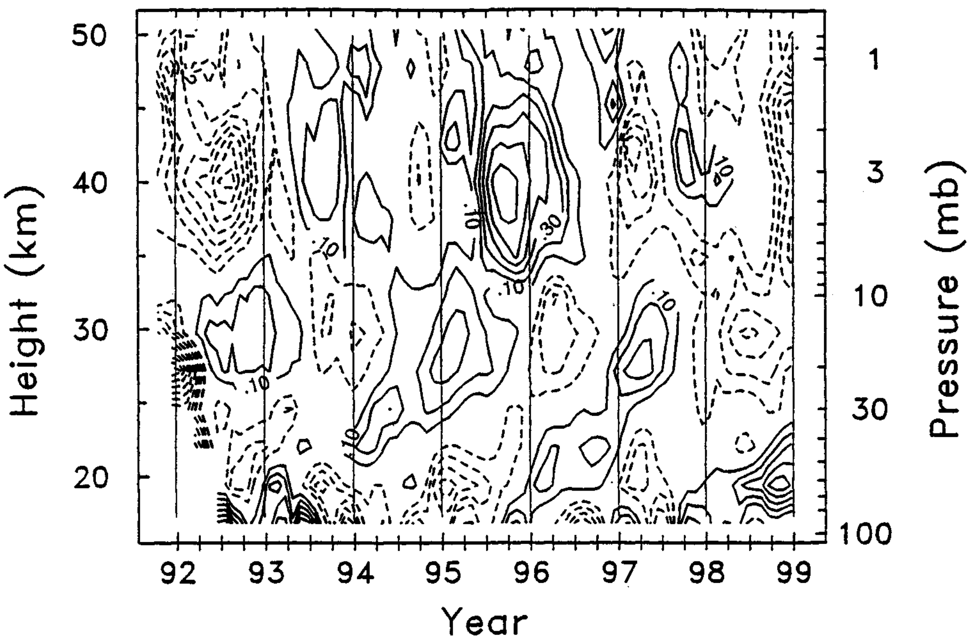

~~Figure 27.~~ Time-height cross sections of interannual anomalies in H_2O over the equator from the Halogen Occultation Experiment (HALOE) instrument. The contour interval is 0.1 ppmv, with 0 contour omitted. Updated from *Randel et al.* [1998].

figure 22.